or somatostatin was detected in livers from wt-PDX1-mice and PDX1-VP16-mice. In addition, in these livers there was no detectable production of amylase, a pancreatic exocrine enzyme (Fig. 2B), which may explain the normal morphogenesis in our experimental animals. On the other hand, pancreatic polypeptide was expressed in livers from PDX1-VP16-mice, and in those from wt-PDX1-mice though to a lesser extent. These results demonstrate that transient expression of PDX1-VP16 alters the character of hepatocytes to preferentially produce insulin and pancreatic polypeptide, but not other endocrine hormones or exocrine enzymes.

Adenoviral gene transfer induced gene expression for 1 week but, after 2 weeks, this expression reportedly disappeared [22]. However, in the present study, the blood glucose lowering effects and hepatic insulin expression persisted for at least 40 days. Therefore, the time course of PDX1 protein expression levels was examined. As shown in Fig. 3A, immunoblotting using anti-VP16 activation domain antibody revealed PDX1-VP16 protein to be expressed on day 3 but expression was markedly decreased on day 7, and undetectable on day 21. Thus, even after disappearance of VP16-PDX1 expression, hepatocytes expressed insulin, resulting in lowering of blood glucose levels. Interestingly, immunoblotting using anti-PDX1 antibody showed that endogenous PDX1 protein, which had the same molecular weight as wt-PDX1, came to be expressed on day 21. Thus, transient expression of PDX1-VP16 endowed hepatocytes with certain pancreatic β cell features and endogenous PDX1 expression is likely to maintain the insulin-producing function of these cells.

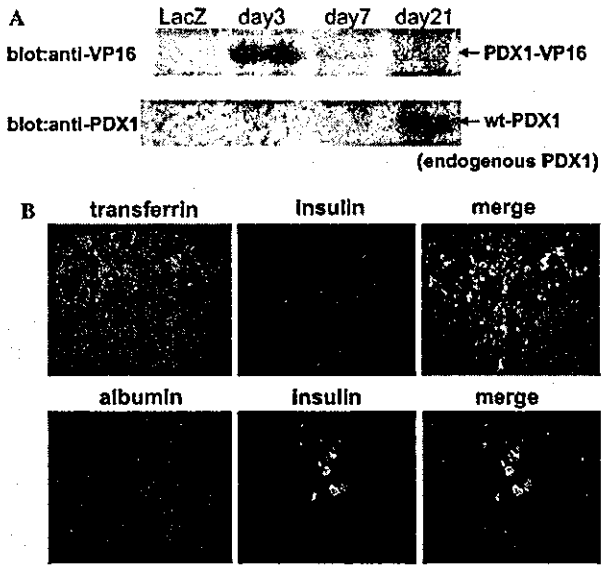

Fig. 3. Treatment with PDX1-VP16 adenovirus induced persistent expression of endogenous PDX1 but albumin and transferrin were co-expressed in insulin-expressing cells. (A) Liver lysates from PDX1-VP16 mice at different time points after adenoviral treatment were immunoblotted with anti-VP16 (upper panel) or anti-PDX1 (lower panel) antibody. (B) Liver sections from PDX1-VP16 mice on day 40 were double-immunostained with insulin (middle panels) and transferrin (upper-left panels) or albumin (lower-left panels) antibodies. Right panels represent the merged images.

To determine whether the insulin-producing cells in the liver had completely transdifferentiated and lost their hepatocytic character, liver sections from PDX1-VP16 mice on day 40 were immunostained with insulin and transferrin (upper panels in Fig. 3B) or albumin (lower panels in Fig. 3B). Fluorescence immunohistochemistry revealed that insulin-producing cells in the liver also expressed transferrin and albumin. Expression levels of these liver-specific proteins were not substantially decreased as compared with non-insulin-producing cells around the insulin-producing cells. These findings suggest functional hepatocyte-specific characteristics are maintained in insulin-producing cells in the liver. Thus, these hepatocytes were not completely converted to pancreatic cells.

Discussion

In the present study, administration of recombinant adenovirus containing an activated form of PDX1 efficiently induced insulin production in hepatocytes, resulting in reversal of STZ-induced hyperglycemia. The effects were sustained even when exogenous protein expression was no longer detectable. In turn, endogenous PDX1 protein came to be expressed in hepatocytes, which is likely to be the mechanism underlying the sustained effects. On the other hand, albumin and transferrin expressions were observed in insulin-producing cells, suggesting the maintenance of hepatocyte-specific characteristics.

Ferber et al. [7] reported that administration of wt-PDX1 adenovirus at 2×10^9 pfu/mouse ameliorates STZ-induced hyperglycemia but the observed period was very short (no more than 10 days). The same research group also reported the long-term effects of PDX1 gene transfer but the titer of recombinant adenovirus used was relatively high ($1–5\times10^{10}$ pfu/mouse) [12]. Such high titers may result in liver damage due to adenoviral toxicity. In the present study, to avoid adenoviral toxicity, recombinant adenoviruses were injected at a titer as low as 2×10^8 pfu. With such a small adenoviral delivery, the wt-PDX1 adenovirus exerted very small effects on insulin and glucose levels, whereas PDX1-VP16 adenovirus substantially increased insulin levels and reversed STZ-induced hyperglycemia. These findings suggest that constitutive activation of PDX1 overcomes the inefficiency associated with low expression levels of PDX1 proteins. Thus, adenoviral transfer of the PDX1-VP16 gene into the liver would presumably be safer than wt-PDX1 gene therapy.

HDAD-mediated PDX1 expression in the liver reportedly causes severe hepatitis including marked inflammatory cell infiltration with focal necrosis associated with expression of pancreatic exocrine genes [10]. In addition, conditional transgenic mice generated by crossing CAG-CAT-PDX1 mice with alb-Cre recombinase-mice also displayed functional liver failure with hepatic expression of exocrine enzymes [11]. In these two models, exogenous PDX1 expression is persistent. Transgenes delivered by HDADs are expressed for long periods exceeding several months. In conditional transgenic mice [11], cells, in which the albumin promoter had once been activated, permanently expressed PDX1 driven by the CAG promoter. These findings suggest that high and persistent expression of PDX1 induces exocrine enzyme expression and thereby liver failure. In the present study, exogenous gene expressions of wt-PDX1 and PDX1-VP16 were transient and expression levels were relatively low on day 7 (Fig. 3A). Thus, transient expression appears to be important for endowing hepatocytes with certain features of pancreatic β cells, but not of exocrine cells.

It is noteworthy that exogenous, transient expression of PDX1-VP16 induced prolonged expression of endogenous PDX1 which apparently contributed to persistent insulin production with hepatocytic features. Ber et al. also reported that rat PDX1 gene transduction using first-generation adenovirus induced persistent endogenous (murine) PDX1 expression. Thus, transient expression of wt-PDX1, and more efficiently PDX1-VP16, may induce persistent and low-level expression of endogenous PDX1. In the adult pancreas, persistent but low-level expression of PDX1 is detected only in β cells [3] and PDX1 expression is required for maintaining normal pancreatic β cell function [6]. These observations suggest that persistent, low-level expression of PDX1 is involved in preferential production of insulin and pancreatic popypeptide in hepatocytes.

In transgenic *Xenopus* tadpoles expressing Xlhbox8 (*Xenopus* homolog of PDX1) carrying the VP16 activation domain under a transthyretin promoter, part or all of the liver is reportedly converted to pancreatic tissue without expression of liver-specific gene products, suggesting complete conversion of hepatocytes to pancreatic cells [14]. In contrast, in the present study, insulin-producing cells in the liver in PDX1-VP16 mice also expressed albumin and transferrin, which suggests preservation of hepatocytic functions. This discrepancy may be explained by the differences between amphibian and mammalian cells. Alternatively, the conversion may occur during embryonic differentiation, while, in adult and differentiated hepatocytes, complete transdifferentiation into pancreatic endocrine or exocrine cells would be difficult to achieve even with PDX1-VP16 expression. Although intensive research is necessary to unravel the precise mechanisms underlying transdifferentiation, the partial conversion induced by PDX1-VP16 expression in adult hepatocytes has practical applications, since loss of hepatocytic functions may result in liver failure. Furthermore, incomplete transdifferentiation could prevent the generated insulin-producing cells from being attacked by a destructive autoimmune response in type 1 diabetics.

Acknowledgments

We thank Dr. H. Kanamori (University of Tokyo) for the generous gift of the VP16 gene. We also thank Ms. I. Sato, K. Kawamura, and M. Hoshi for technical support. This work was supported by a Grant-in-Aid for Scientific Research (B2, 15390282), a Grant-in-Aid for Exploratory Research (15659214) to H. Katagiri, and a Grant-in-Aid for Scientific Research (13204062) to Y. Oka from the Ministry of Education, Science, Sports and Culture of Japan. This work was also supported by Tohoku University 21st Century COE Program "CRESCENDO" to J. Imai, J. Gao, and H. Katagiri.

References

[1] A.M. Shapiro, J.R. Lakey, E.A. Ryan, G.S. Korbutt, E. Toth, G.L. Warnock, N.M. Kneteman, R.V. Rajotte, Islet transplantation in seven patients with type 1 diabetes mellitus using a glucocorticoid-free immunosuppressive regimen, N. Engl. J. Med. 343 (2000) 230–238.

[2] G. Deutsch, J. Jung, M. Zheng, J. Lora, K.S. Zaret, A bipotential precursor population for pancreas and liver within the embryonic endoderm, Development 128 (2001) 871–881.

[3] H. Ohlsson, K. Karlsson, T. Edlund, Ipf1, a homeodomain-containing transactivator of the insulin gene, EMBO J. 12 (1993) 4251–4259.

[4] M.F. Offield, T.L. Jetton, P.A. Labosky, M. Ray, R.W. Stein, M.A. Magnuson, B.L. Hogan, C.V. Wright, Pdx-1 is required for pancreatic outgrowth and differentiation of the rostral duodenum, Development 122 (1996) 983–995.

[5] J. Jonsson, L. Carlsson, T. Edlund, H. Edlund, Insulin-promoter-factor 1 is required for pancreas development in mice, Nature 371 (1994) 606–609.

[6] U. Ahlgren, J. Jonsson, L. Jonsson, K. Simu, H. Edlund, Beta-cell-specific inactivation of the mouse ipf1/pdx1 gene results in loss of the beta-cell phenotype and maturity onset diabetes, Genes Dev. 12 (1998) 1763–1768.

[7] S. Ferber, A. Halkin, H. Cohen, I. Ber, Y. Einav, I. Goldberg, I. Barshack, R. Seijffers, J. Kopolovic, N. Kaiser, A. Karasik, Pancreatic and duodenal homeobox gene 1 induces expression of insulin genes in liver and ameliorates streptozotocin-induced hyperglycemia, Nat. Med. 6 (2000) 568–572.

[8] A. Grapin-Botton, A.R. Majithia, D.A. Melton, Key events of pancreas formation are triggered in gut endoderm by ectopic expression of pancreatic regulatory genes, Genes Dev. 15 (2001) 444–454.

[9] R.S. Heller, D.A. Stoffers, M.A. Hussain, C.P. Miller, J.F. Habener, Misexpression of the pancreatic homeodomain protein idx-1 by the hoxa-4 promoter associated with agenesis of the cecum, Gastroenterology 115 (1998) 381–387.

[10] H. Kojima, M. Fujimiya, K. Matsumura, P. Younan, H. Imaeda, M. Maeda, L. Chan, Neurod-betacellulin gene therapy induces islet neogenesis in the liver and reverses diabetes in mice, Nat. Med. 9 (2003) 596–603.
[11] T. Miyatsuka, H. Kaneto, Y. Kajimoto, S. Hirota, Y. Arakawa, Y. Fujitani, Y. Umayahara, H. Watada, Y. Yamasaki, M.A. Magnuson, J. Miyazaki, M. Hori, Ectopically expressed pdx-1 in liver initiates endocrine and exocrine pancreas differentiation but causes dysmorphogenesis, Biochem. Biophys. Res. Commun. 310 (2003) 1017–1025.
[12] I. Ber, K. Shternhall, S. Perl, Z. Ohanuna, I. Goldberg, I. Barshack, L. Benvenisti-Zarum, I. Meivar-Levy, S. Ferber, Functional, persistent, and extended liver to pancreas transdifferentiation, J. Biol. Chem. 278 (2003) 31950–31957.
[13] S. Dutta, M. Gannon, B. Peers, C. Wright, S. Bonner-Weir, M. Montminy, Pdx:Pbx complexes are required for normal proliferation of pancreatic cells during development, Proc. Natl. Acad. Sci. USA 98 (2001) 1065–1070.
[14] M.E. Horb, C.N. Shen, D. Tosh, J.M. Slack, Experimental conversion of liver to pancreas, Curr. Biol. 13 (2003) 105–115.
[15] H. Mizuguchi, M.A. Kay, Efficient construction of a recombinant adenovirus vector by an improved in vitro ligation method, Hum. Gene Ther. 9 (1998) 2577–2583.
[16] H. Mizuguchi, M.A. Kay, A simple method for constructing e1- and e1/e4-deleted recombinant adenoviral vectors, Hum. Gene Ther. 10 (1999) 2013–2017.
[17] T. Anno, S. Uehara, H. Katagiri, Y. Ohta, K. Ueda, H. Mizuguchi, Y. Moriyama, Y. Oka, Y. Tanizawa, Overexpression of constitutively activated glutamate dehydrogenase induces insulin secretion through enhanced glutamate oxidation, Am. J. Physiol. Endocrinol. Metab. 286 (2004) E280–E285.
[18] H. Katagiri, T. Asano, H. Ishihara, K. Inukai, Y. Shibasaki, M. Kikuchi, Y. Yazaki, Y. Oka, Overexpression of catalytic subunit p110alpha of phosphatidylinositol 3-kinase increases glucose transport activity with translocation of glucose transporters in 3t3-l1 adipocytes, J. Biol. Chem. 271 (1996) 16987–16990.
[19] I. Sadowski, J. Ma, S. Triezenberg, M. Ptashne, Gal4-vp16 is an unusually potent transcriptional activator, Nature 335 (1988) 563–564.
[20] S.J. Triezenberg, R.C. Kingsbury, S.L. McKnight, Functional dissection of vp16, the trans-activator of herpes simplex virus immediate early gene expression, Genes Dev. 2 (1988) 718–729.
[21] Y. Ishigaki, S. Oikawa, T. Suzuki, S. Usui, K. Magoori, D.H. Kim, H. Suzuki, J. Sasaki, H. Sasano, M. Okazaki, T. Toyota, T. Saito, T.T. Yamamoto, Virus-mediated transduction of apolipoprotein e (apoe)-sendai develops lipoprotein glomerulopathy in apoe-deficient mice, J. Biol. Chem. 275 (2000) 31269–31273.
[22] M.J. Peeters, G.A. Patijn, A. Lieber, L. Meuse, M.A. Kay, Adenovirus-mediated hepatic gene transfer in mice: comparison of intravascular and biliary administration, Hum. Gene Ther. 7 (1996) 1693–1699.

Diabetologia (2004) 47:794–805
DOI 10.1007/s00125-004-1391-x

Diabetologia

Oxidative stress induces insulin resistance by activating the nuclear factor-κB pathway and disrupting normal subcellular distribution of phosphatidylinositol 3-kinase

T. Ogihara[1,2] · T. Asano[1] · H. Katagiri[2] · H. Sakoda[3] · M. Anai[3] · N. Shojima[1] · H. Ono[3] · M. Fujishiro[1] · A. Kushiyama[1] · Y. Fukushima[1] · M. Kikuchi[3] · N. Noguchi[4] · H. Aburatani[4] · Y. Gotoh[5] · I. Komuro[6] · T. Fujita[1]

[1] Department of Internal Medicine, Graduate School of Medicine, University of Tokyo, Tokyo, Japan
[2] Division of Advanced Therapeutics for Metabolic Diseases, Center for Translational and Advanced Animal Research on Human Diseases, Tohoku University Graduate School of Medicine, Sendai, Japan
[3] The Institute for Adult Diseases, Asahi Life Foundation, Tokyo, Japan
[4] Research Center for Advanced Science and Technology, University of Tokyo, Tokyo, Japan
[5] Department of Molecular Biology, Institute of Molecular and Cellular Biosciences, University of Tokyo, Tokyo, Japan
[6] Department of Cardiovascular Science and Medicine, Chiba University Graduate School of Medicine, Chiba, Japan

Abstract

Aims/hypothesis. Oxidative stress is associated with diabetes, hypertension and atherosclerosis. Insulin resistance is implicated in the development of these disorders. We tested the hypothesis that oxidative stress induces insulin resistance in rats, and endeavoured to identify mechanisms linking the two.
Methods. Buthionine sulfoximine (BSO), an inhibitor of glutathione synthase, was administered to Sprague-Dawley rats and 3T3-L1 adipocytes. Glucose metabolism and insulin signalling both in vivo and in 3T3-L1 adipocytes were examined. In 3T3-L1 adipocytes, the effects of overexpression of a dominant negative mutant of inhibitory κB (IκB), one role of which is to block oxidative-stress-induced nuclear factor (NF)-κB activation, were investigated.
Results. In rats given BSO for 2 weeks, the plasma lipid hydroperoxide level doubled, indicating increased oxidative stress. A hyperinsulinaemic-euglycaemic clamp study and a glucose transport assay using isolated muscle and adipocytes revealed insulin resistance in BSO-treated rats. BSO treatment also impaired insulin-induced glucose uptake and GLUT4 translocation in 3T3-L1 adipocytes. In BSO-treated rat muscle, adipose tissue and 3T3-L1 adipocytes, insulin-induced IRS-1 phosphorylation in the low-density microsome (LDM) fraction was specifically decreased, while that in whole cell lysates was not altered, and subsequent translocation of phosphatidylinositol (PI) 3-kinase from the cytosol and the LDM fraction was disrupted. BSO-induced impairments of insulin action and insulin signalling were reversed by overexpressing the dominant negative mutant of IκB, thereby suppressing NF-κB activation.
Conclusions/interpretation. Oxidative stress induces insulin resistance by impairing IRS-1 phosphorylation and PI 3-kinase activation in the LDM fraction, and NF-κB activation is likely to be involved in this process.

Keywords Buthionine sulfoximine · Glutathione · Hyperinsulinaemic-euglycaemic clamp · Inhibitory κB · Insulin resistance · IRS · Nuclear factor-κB · Oxidative stress · Phosphatidylinositol 3-kinase

Received: 20 October 2003 / Accepted: 26 January 2004
Published online: 1 May 2004

T. Asano (✉)
Department of Internal Medicine, Graduate School of Medicine, University of Tokyo, Tokyo 113-8655, Japan
E-mail: asano-tky@umin.ac.jp
Tel.: +81-3-38153411 ext. 33133, Fax: +81-3-58031874

Present address:
T. Asano
Department of Physiological Chemistry and Metabolism, Graduate School of Medicine, University of Tokyo, Tokyo 113-8655, Japan

Introduction

Oxidative stress represents an imbalance between production of reactive oxygen species and the antioxidant defence system [1]. Oxidative stress is widely recognised as being associated with various disorders including diabetes, hypertension and atherosclerosis. In-

Abbreviations: BSO, buthionine sulfoximine · GMSA, gel mobility shift assay · IκB, inhibitory κB · IKK, IκB kinase · LDM, low-density microsome · NF-κB, nuclear factor-κB · PI, phosphatidylinositol

sulin resistance is a common feature of these disorders [2, 3]. Indeed, in diabetic people and in animal models of diabetes, the plasma free radical concentration is increased [4, 5] and antioxidant defences are diminished [6, 7]. It has also been suggested that antioxidant agents such as vitamin C [8] and E [9] improve insulin action in diabetic subjects.

Angiotensin II reportedly induces free radical production and increases plasma oxidative stress [10]. In our previous study, we showed continuous infusion of angiotensin II to induce insulin resistance with increased oxidative stress in rats, while the spin trap agent tempol [11], which works as a superoxide dismutase mimetic, decreases oxidative stress and improves insulin resistance in these rats [12]. A similar coexistence of oxidative stress and insulin resistance, as well as recovery with tempol administration was observed in adrenomedullin-deficient mice [13]. These previous reports strongly suggest a close relationship between oxidative stress and insulin resistance. Thus, we attempted to elucidate the molecular mechanisms underlying insulin resistance and oxidative stress.

In this study, to increase oxidative stress in vivo, we utilised a selective inhibitor of γ-glutamylcysteine synthetase, i.e. an inhibitor of glutathione synthase, buthionine sulfoximine (BSO). Glutathione is one of the major components of the antioxidant defence system, such that BSO administration increases oxidative stress by reducing the tissue glutathione level [14]. Although BSO does not have toxic effects in animals [14], BSO-treated rats were previously shown to exhibit glucose intolerance [15] and hypertension [16]. In the current study, we examined the effect of BSO treatment on insulin resistance in rats and 3T3-L1 adipocytes. We investigated the molecular mechanisms underlying BSO-induced insulin resistance, focusing on the subcellular distribution of phosphatidylinositol (PI) 3-kinase. Finally, we examined the involvement of the nuclear factor (NF)-κB pathway in BSO-induced insulin resistance and insulin signalling impairment.

Materials and methods

Materials. Affinity-purified antibodies against IRS-1 and GLUT4 were prepared as previously described [17]. Antibodies against phosphotyrosine, the p85 subunit of PI 3-kinase, and inhibitory κB (IκB) were purchased from Upstate Biotechnology (Milton Keynes, UK). TNF-α and buthionine-[S, R]-sulfoximine (BSO) were purchased from Sigma-Aldrich (St. Louis, Mo., USA).

Animals. Seven-week-old male Sprague-Dawley rats (Tokyo Experimental Animals, Tokyo, Japan) were fed a standard rodent diet with or without water containing 30 mmol/l BSO for 14 days [16]. The animal care was in accordance with the policies of the University of Tokyo, and the "Principles of laboratory animal care" (NIH publication no. 85-23, revised 1985) were followed.

Measurements. Cholesteryl ester hydroperoxides were analysed by HPLC, with 234 nm UV detection and post-column chemiluminescence detection on an LC-8 column (Supelco, 4×250 mm, 5-μm particles; Sigma-Aldrich) and methanol/tert-butyl alcohol (95/5 vol) as the eluent, as reported previously but with slight modification [18]. In brief, plasma was extracted with 10 volumes of methanol and 50 volumes of hexane. The hexane phase was removed, dried under N_2 gas and redissolved in an eluent for HPLC injection. Liver glutathione content was measured spectrophotometrically using a glutathione reductase recycling assay, as described previously [19].

Hyperinsulinaemic-euglycaemic clamp study. Rats fasted overnight were anaesthetised by intraperitoneal injection of pentobarbital sodium (60 mg/kg body weight) and the left jugular and femoral veins were catheterised for blood sampling and infusion respectively. Hyperinsulinaemic-euglycaemic clamp analysis was performed as described previously [17]. The glucose utilisation rate, hepatic glucose production and an estimate of muscle glucose uptake during the clamp (defined as the glucose metabolic index) were calculated as previously described [20].

Glucose uptake into isolated soleus muscle. Rats fasted overnight were anaesthetised and soleus muscles were dissected out and rapidly cut into 20–40 mg strips. The rats were then killed by intracardiac injection of pentobarbital. Isolated soleus muscle was incubated for 20 min with or without 1.44×10^{-8} mol/l human insulin (this concentration is equivalent to 2 mU/ml), as described previously [17]. 2-Deoxy glucose uptake into the isolated soleus muscle strips was measured using 2-deoxy-D-[^{3}H]glucose and [^{14}C]manitol as described previously [21].

Preparation of rat adipocytes and measurement of glucose uptake. Isolated rat adipocytes were prepared from epididymal adipose tissue harvested from fasted rats using the collagenase method [22], and 2-deoxy glucose uptake was then assayed as previously described [23].

Adenovirus-mediated gene transfer to 3T3-L1 adipocytes. 3T3-L1 fibroblasts were maintained in DMEM supplemented with 10% donor calf serum and differentiated into adipocytes as previously described [24]. The dominant negative mutant of IκB-α, in which serine residues 32 and 36 were substituted with alanine, was kindly provided by Dr R. Gaynor (University of Texas Southwestern Medical Center at Dallas, Tex., USA). To obtain recombinant adenovirus, pAdeno-X was ligated with cDNA encoding *Escherichia coli* lacZ and dominant negative IκB according to the manufacturer's instructions for the Adeno-X Expression System (Clontech, Palo Alto, Calif., USA). Infection of 3T3-L1 adipocytes with the adenovirus was carried out as described previously [25]. Recombinant adenoviruses were applied at a multiplicity of infection of approximately 200–300 pfu/cell and 3T3-L1 adipocytes infected with lacZ virus were used as a control.

Gel mobility shift assay. Nuclear protein extracts from 3T3-L1 adipocytes were prepared using NE-PER nuclear and cytoplasmic extraction reagents (Pierce Biotechnology, Rockford, Ill., USA) according to the manufacturer's instructions and used for gel mobility shift assay (GMSA). Briefly, 3T3-L1 adipocytes were homogenised in 1 ml of PBS and centrifuged for 10 min at 500 × *g* at 4 °C. After removing the supernatant, the pellet was resuspended in 500 μl of Cytoplasmic Extraction Reagent I buffer containing protease inhibitors (1 600 mol/l benzamidine, 0.3 mmol/l aprotinin, 4.2 mol/l leupeptin, 0.2 mol/l phenylmethylsulfonyl fluoride), and was incubated

on ice for 10 min. Then, 27.5 µl of Cytoplasmic Extraction Reagent II buffer were added to the sample, which was vortexed and centrifuged at 16 000 × *g* for 5 min. The resultant pellet was resuspended in 250 µl of NER buffer, vortexed every 10 minutes for 40 min and then centrifuged at 16 000 × *g* for 10 min. The supernatant containing nuclear proteins was stored at –80 °C. For the GMSA, 10 µg of nuclear proteins were incubated in binding buffer with 3.5 pmol of double-stranded DNA oligonucleotide containing an NF-κB consensus-binding sequence labelled with [^{32}P]-ATP using T4 polynucleotide kinase for 30 min at 37 °C. For supershift analyses, monoclonal antibody against NF-κB p65 was separately pre-incubated with nuclear extracts at 4 °C for 20 min in a total volume of 16 µl of binding buffer, followed by incubation with 8 µl of ^{32}P-labelled oligonucleotide probe with and without cold oligonucleotide probe at 4 °C for 20 min using a Nushift Kit (Geneka Biotechnology, Carlsbad, Calif., USA). Protein-DNA complexes were separated from the unbound DNA probe by electrophoresis through 5% polyacrylamide gels containing 1× Tris-glycine-EDTA buffer. The gel was dried and exposed to BAS2000 (Fujifilm, Tokyo, Japan).

Glucose uptake into 3T3-L1 adipocytes. 3T3-L1 adipocytes plated in 24-well culture dishes were serum starved for 3 h in DMEM containing 0.2% bovine serum albumin, after which they were incubated in Krebs–Ringer phosphate buffer for an additional 45 min, prior to incubation with or without 10^{-6} or 10^{-7} mol/l insulin for 15 min. The assay was initiated by adding 2-deoxy-D-[^{3}H]glucose (1.85×10^{7} Bq/sample, 0.1 mmol) and was terminated 4 min later by washing the cells once with ice-cold Krebs–Ringer phosphate buffer containing 0.3 mmol/l phloretin and then twice with ice-cold Krebs–Ringer phosphate buffer. The cells were then solubilised in 0.1% SDS, and the incorporated radioactivity was determined by scintillation counting [26].

Subcellular fractionation. 3T3-L1 adipocytes were serum starved for 3 h and incubated with or without 10^{-6} mol/l insulin for 15 min. Cells were fractionated as described previously [27]. Briefly, 3T3-L1 adipocytes were resuspended in HES buffer (255 mmol/l sucrose, 20 mmol/l HEPES [pH 7.4], 1 mmol/l EDTA), homogenised and subjected to differential centrifugation. The supernatants from the following spins were serially removed and pelleted in a Ti70 rotor as follows: 19 000 × *g* (20 min), 41 000 × *g* (20 min) and 180 000 × *g* (75 min). The first 19 000 × *g* pellet was resuspended, loaded onto a sucrose cushion (1.12 mol/l sucrose, 20 mmol/l HEPES [pH 7.4], 1 mmol/l EDTA) and isolated from the interface yielding the plasma membrane fraction as the pellet of a 41 000 × *g* spin (20 min). The last 180 000 × *g* pellet corresponded to the low-density microsome (LDM) fraction. Subcellular fractionation and measurement of GLUT4 translocation in isolated skeletal muscle and adipocytes from rats were described previously [12]. After resuspension of the pellets in solubilisation buffer, 20 µg of each fraction were loaded for western blotting. Proteins in the plasma membrane and LDM fractions were separated by SDS-PAGE, transferred to a polyvinylidene fluoride membrane, immunoblotted with anti-GLUT4, anti-IRS-1 or anti-p85 antibodies, and reacted with enhanced chemiluminescence reagent (Amersham Biosciences, Uppsala, Sweden) or subject to immunoprecipitation and PI 3-kinase assay of the immunoprecipitates as previously described [17].

Immunoprecipitation and immunoblotting. In rat experiments, rats fasted overnight were anaesthetised, and within 10–15 min the abdominal cavity was opened, the portal vein exposed, and 16 ml/kg body weight of normal saline (0.9% NaCl), with or without 10^{-5} mol/l human insulin, were injected. After 60 s, hindlimb muscles were removed and immediately homogenised as described previously [28]. In 3T3-L1 experiments, 3T3-L1 adipocytes were serum-starved for 18 h, pre-incubated with or without 80 µmol/l BSO for 18 h, then stimulated with or without 10^{-6} mol/l insulin for 15 min. The cells were then washed and lysed with lysis buffer as described previously [29]. After centrifugation, the resultant supernatants were used for immunoprecipitation or immunoblotting as described previously [28]. Proteins were visualised with enhanced chemiluminescence and band intensities were quantified with a Molecular Imager GS-525 using Imaging Screen-CH (Bio-Rad Laboratories, Hercules, Calif., USA). In some experiments, 3T3-L1 cells were incubated with 5.8 pmol/l (equivalent to 10 ng/dl) TNF-α or 80 µmol/l BSO for 18 h, lysed and immunoblotted with anti-IκB antibody.

Phosphatidylinositol 3-kinase activity. After preparing tissue samples as above, IRS-1 was immunoprecipitated, and PI 3-kinase activity in the immunoprecipitates was assayed as previously described [17].

Statistical analysis. Data are expressed as means ± SE. Comparisons between the two groups were made using unpaired *t* tests. We considered *p* values of less than 0.05 to be statistically significant.

Results

Characterisation of rats studied. Although food intakes were similar in the two groups, the BSO-treated rats had lower body weights than control rats (Table 1). Individual water consumptions did not differ between the two. Systolic and diastolic blood pressures were similar in the two groups of rats. Fasting blood glucose and plasma insulin levels in BSO rats were also similar to those of control rats. Although fasting insulin levels were not elevated in BSO-treated rats as compared with those of controls, we found that

Table 1. Characterisation of BSO-treated rats

	Control	BSO
Body weight (g)	320.0±8.7	284±4.1*
Food intake (g/day)	20.2±2.4	21.2±2.3
Water intake (ml/day)	38.2±1.8	36.8±3.2
Systolic BP (mm Hg)	113.5±4.4	120.7±3.9
Diastolic BP (mm Hg)	83.4±4.4	87.8±1.4
Fasting blood glucose (mmol/l)	6.12±0.32	6.32±0.24
Randomly fed blood glucose (mmol/l)	8.37±0.24	8.44±0.17
Fasting plasma insulin (pmol/l)	109±16	112±3
Randomly fed plasma insulin (pmol/l)	188±17	367±3*
Glutathione content of liver (µmol/g tissue)	3.2±0.3	1.1±0.4*
Plasma cholesteryl ester hydroperoxide (mmol/l)	1.38±0.3	2.72±0.3*

Data are means ± SE; rats in each group, n=6; * p<0.05 compared with controls

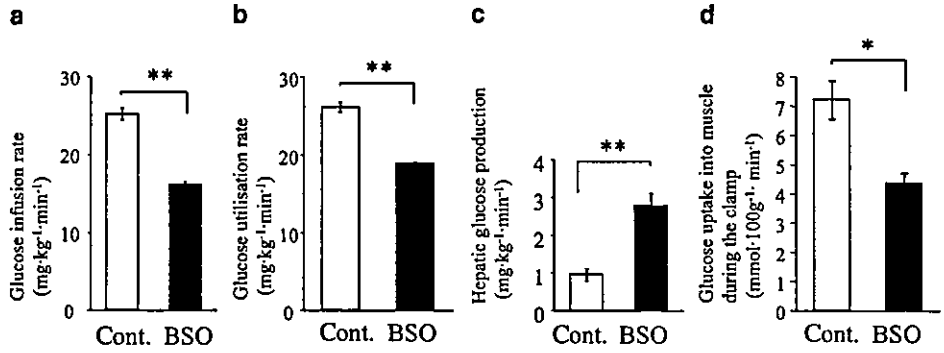

Fig. 1. A hyperinsulinaemic-euglycaemic clamp study. Rats were anaesthetised by intraperitoneal injection of pentobarbital sodium and the left jugular and femoral veins were catheterised for blood sampling and infusion respectively. Hyperinsulinaemic-euglycaemic clamp analysis was performed as described previously [17]. The glucose infusion rate (**a**), glucose utilisation rate (**b**), hepatic glucose production (**c**) and muscle glucose uptake during the clamp (defined as the glucose metabolic index; **d**) were estimated from hyperinsulinaemic-euglycaemic clamp data. * $p<0.05$, ** $p<0.01$ compared with the control. Bars represent the means ± SE of results from four to five rats. Cont. indicates control Sprague-Dawley rats. BSO indicates rats fed a standard rodent diet with water containing 30 mmol/l BSO for 12 days

among well-fed animals, insulin levels in BSO-treated rats were significantly higher than those in controls. To determine the effect of BSO as a glutathione synthase inhibitor, hepatic glutathione content was measured, because glutathione is most abundant in the liver. The glutathione level was significantly lower, by 34%, in the livers of BSO-treated rats than in those of controls. The cholesteryl ester hydroperoxide level in BSO-treated rat plasma was double that in control rats, suggesting that oxidative stress is increased in BSO-treated rats.

Hyperinsulinaemic-euglycaemic clamp study. Whole-body insulin sensitivity was evaluated using a hyperinsulinaemic-euglycaemic clamp technique. Compared with controls, the glucose infusion rate was decreased by 36.2% and the glucose utilisation rate by 27.6% during submaximal insulin infusion in BSO-treated rats (Figs. 1a, b). In addition, hepatic glucose production was increased by 29.3% in BSO-treated rats, suggesting impairment of the ability of insulin to suppress hepatic glucose production (Fig. 1c). Glucose uptake into skeletal muscle during the clamp was decreased by 39.4% in BSO-treated rats (Fig. 1d). These results suggest that BSO treatment induces insulin resistance both systemically and in skeletal muscle and liver.

Insulin-induced glucose uptake and GLUT4 translocation in BSO-treated rat skeletal muscle and adipocytes. In BSO-treated rats, insulin-induced glucose uptakes into isolated soleus muscle and adipocytes were reduced by 21.4% and 47.8% respectively as compared with the control levels (Figs. 2a, c). Subsequent western blot analysis showed the GLUT4 contents of skeletal muscle and adipocytes to be similar in the two groups (Figs. 2b, d, upper panels), indicating that the impairment of insulin-induced glucose uptake in these tissues from BSO-treated rats was not due to reduced expression of GLUT4 proteins. However, insulin-induced GLUT4 translocation, as assessed by the appearance of GLUT4 in the plasma membrane fraction of skeletal muscle and adipose tissue, was decreased in BSO-treated rats (Figs. 2b, d, lower panels). Microscopic analysis revealed adipocytes from BSO-treated rats to be small, which is consistent with the low body weights of these rats (Fig. 2e), suggesting that insulin resistance in BSO-treated rats is not attributable to adipocyte enlargement.

Impairment of insulin signalling in BSO-treated rat skeletal muscle and adipocytes. Next, we investigated insulin-induced tyrosine phosphorylation of IRS-1, association of PI 3-kinase with IRS-1, and PI 3-kinase activation in skeletal muscle and adipose tissue in vivo by injecting insulin through the portal vein of anaesthetised rats. Protein amount and insulin-induced tyrosine phosphorylation of IRS-1 in skeletal muscle (whole tissue lysates) from BSO-treated rats were similar to those in controls (Fig. 3a, upper panels). Because the insulin signalling in the LDM fraction has been implicated in several insulin actions including insulin-induced glucose uptake [30, 31], we carried out subcellular fractionation studies of skeletal muscles from these rats. Subcellular fractionation data showed insulin-induced tyrosine phosphorylation of IRS-1 in the LDM fraction to be significantly decreased in BSO-treated rats as compared with controls, although the IRS-1 protein amount in this fraction was unchanged (Fig. 3a, upper panels). In the cytosol, the amount of IRS-1 and insulin-induced phosphorylation were similar in BSO-treated and control rat muscles (Fig. 3a, upper panels). Next, we investigated the amount of the p85 subunit for PI 3-kinase protein in whole tissue lysates, the LDM fraction and the cytosol (Fig. 3a, middle panels). The amounts of p85 protein were similar in whole tissue

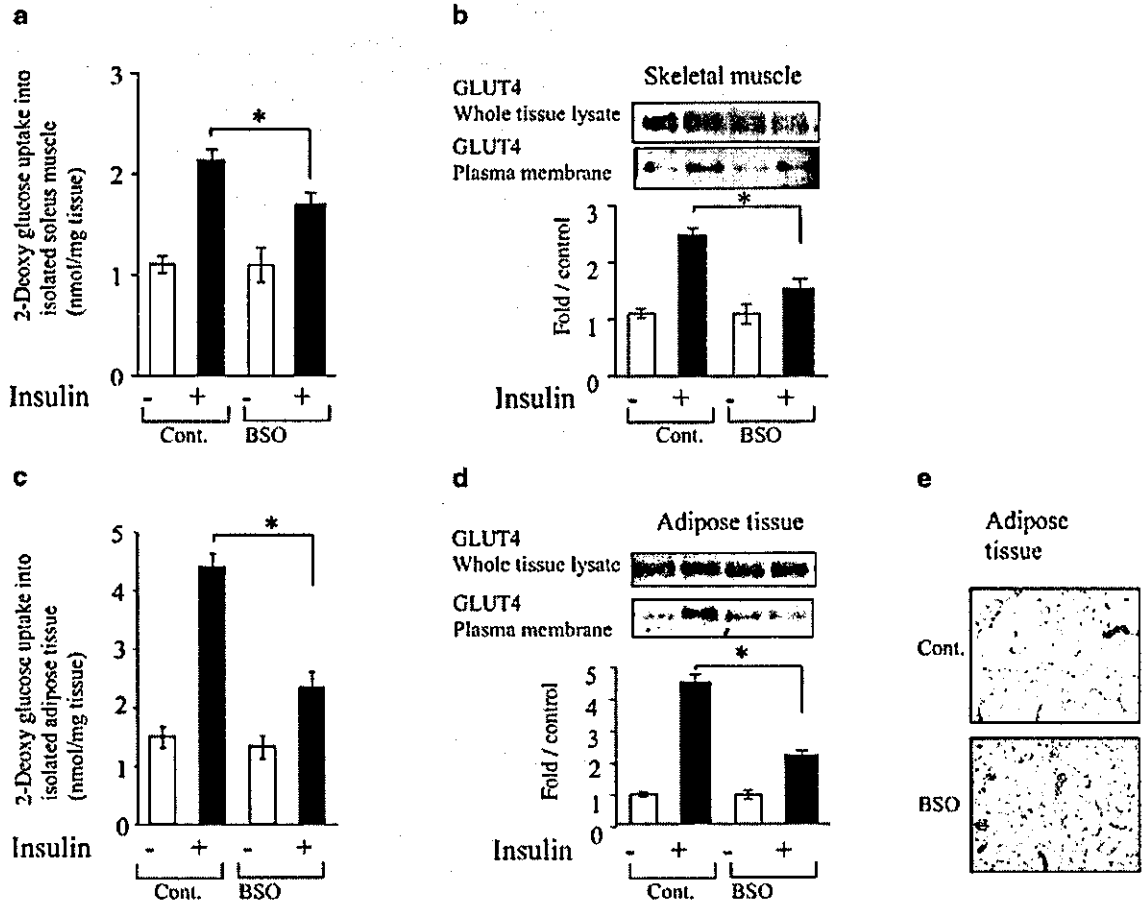

Fig. 2. Insulin resistance in isolated skeletal muscle and adipose tissue in BSO-treated rats. **a.** 2-Deoxy-glucose uptakes into isolated soleus muscle and adipose tissue (**c**). Isolated rat soleus muscle was incubated for 20 min with or without 1.44×10^{-8} mol/l human insulin (this concentration is equivalent to 2 mU/ml) as described previously [17]. 2-Deoxy-D-[1-^{3}H]glucose uptake into the isolated soleus muscle strips was measured as described previously [21]. Isolated rat adipocytes were prepared from epididymal adipose tissue harvested from fasted rats using the collagenase method [22], and 2-deoxy glucose uptake was then assayed as previously described [23]. **b, d.** GLUT4 protein amount in whole tissue lysates (upper panels), the plasma membrane fraction (lower panels) of skeletal muscle (**b**) and adipose tissue (**d**) under basal or insulin-stimulated conditions. Subcellular fractionation and measurement of GLUT4 translocation of isolated skeletal muscle and adipocytes from rats were described previously [12]. Whole tissue lysates and plasma membrane fractions were subjected to SDS-PAGE followed by immunoblotting with anti-GLUT4 antibody. The data are representative of three independent experiments. Bars depict means ± SE of the results from four to six samples. * $p<0.05$ compared with the control under the insulin-stimulated conditions. **d.** Haematoxylin and eosin stained adipose tissues from control and BSO-treated rats are shown. Cont. indicates control Sprague-Dawley rats. BSO indicates rats fed a standard rodent diet with water containing 30 mmol/l BSO for 12 days

lysates before and after insulin stimulation. However, insulin stimulation induced a p85 increase in the LDM fraction and a decrease in the cytosol, suggesting that insulin stimulates p85 translocation from the cytosol to the LDM fraction. This insulin-induced translocation of p85 was disrupted in BSO-treated rats. Insulin-induced increases in IRS-1-associated p85 protein and PI 3-kinase activity did not differ significantly between whole tissue lysates and the cytosol in either BSO-treated or control rat muscle (Fig. 3a, lower panels). However, both were significantly decreased in the LDM fraction of BSO-treated rats as compared with the controls. We obtained essentially the same results in the adipose tissue of these rats (Fig. 3b). In addition, we confirmed that insulin-induced tyrosine phosphorylation of the insulin receptor and IRS-2, as well as Ser-473 phosphorylation of Akt, in the whole tissue lysates of skeletal muscle and adipose tissue does not differ between BSO-treated and control rats (data not shown). Thus, early insulin-signalling steps were shown to be impaired specifically in the LDM fraction, but not in whole tissue lysates of skeletal muscle and adipose tissue from BSO-treated rats.

Insulin action and insulin signalling in BSO-treated 3T3-L1 adipocytes. To further investigate the impaired step in BSO-induced insulin resistance, 3T3-L1

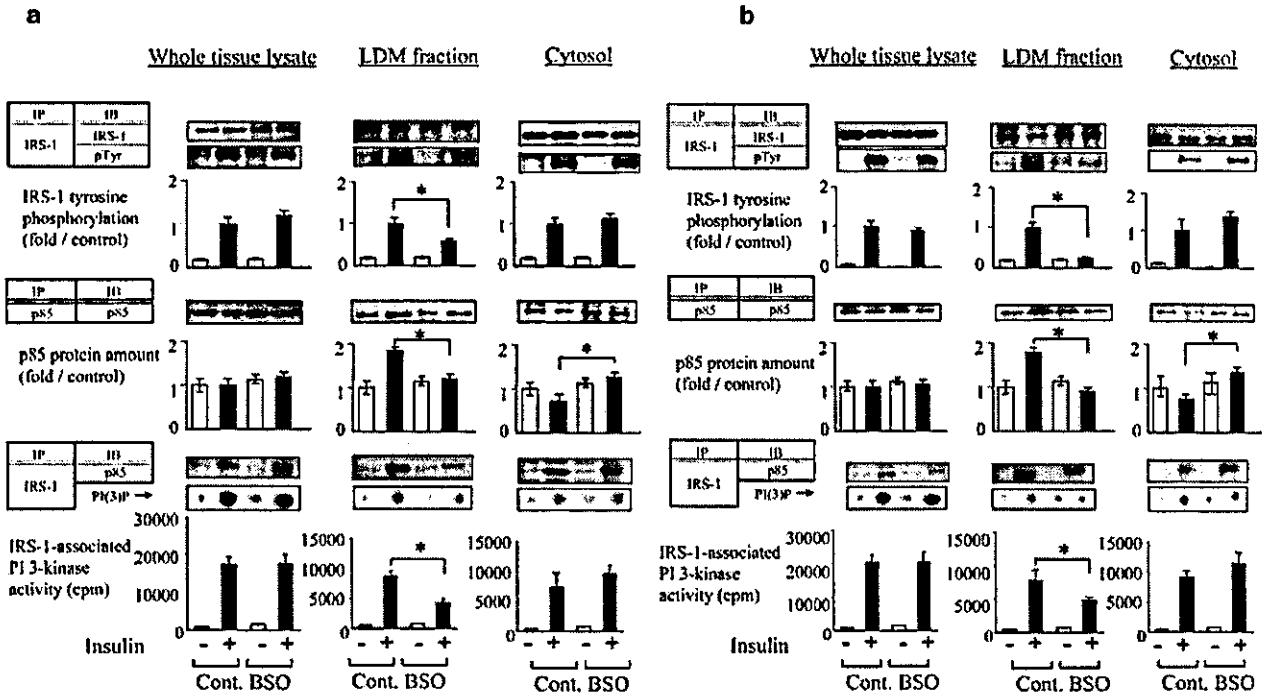

Fig. 3. Insulin signalling in skeletal muscle (**a**) and adipose tissue (**b**) from BSO-treated rats. Rats were anaesthetised, the portal vein exposed, and 16 ml/kg body weight of normal saline, with or without 10^{-5} mol/l human insulin, were injected. After 60 s, hindlimb muscles and epididymal fat were removed and immediately homogenised as described previously [28]. After centrifugation, the resultant supernatants were employed for immunoprecipitation or immunoblotting using the indicated antibodies as described previously [28]. Proteins were visualised with enhanced chemiluminescence and band intensities were quantified with a Molecular Imager GS-525 using Imaging Screen-CH (Bio-Rad). Bars depict means ± SE of the quantitated tyrosine phosphorylation bands, independently obtained in triplicate. Representative spots of PI(3)P are shown in the lower panels and bars depict means ± SE of PI 3-kinase activity measured in three independent assays. * $p<0.05$ compared with the control under the insulin-stimulated condition. IP, immunoprecipitation; IB, immunoblotting; pTyr, phosphotyrosine

adipocytes were incubated with 80 μmol/l BSO for 18 h [32]. It was reported that BSO treatment of adipocytes markedly decreases cellular glutathione levels and increases reactive oxygen species [15, 32]. Incubation with BSO did not affect the morphology or the viability of 3T3-L1 adipocytes (data not shown). Insulin-induced glucose uptake into 3T3-L1 adipocytes was decreased by 42.5% in BSO-treated cells (Fig. 4a). In these cells, insulin-induced GLUT4 translocation to the plasma membrane was impaired (Fig. 4b). Next, we determined insulin-induced IRS-1 phosphorylation and PI 3-kinase activation in whole cell lysates, the LDM fraction and the cytosol. As in rats, protein levels and insulin-induced tyrosine phosphorylations of IRS-1 and IRS-1-associated PI 3-kinase were unaffected by BSO treatment (Fig. 4c, upper panel). In control cells and in BSO-treated cells, p85 protein levels did not differ before versus after insulin stimulation. Next, we examined IRS-1 tyrosine phosphorylation and IRS-1 associated PI 3-kinase activity in the LDM fraction and the cytosol. While IRS-1 protein levels did not change after incubation with BSO, insulin-induced IRS-1 tyrosine phosphorylation in the LDM fraction was suppressed by BSO treatment (Fig. 4c, middle panel). The amount of p85 protein was increased in the LDM fraction and decreased in the cytosol after insulin stimulation, indicating that insulin induces p85 translocation from the cytosol to the LDM fraction in control cells. However, the p85 increase in the LDM fraction was clearly disrupted in BSO-treated cells (Fig. 4c, middle panel). In parallel, insulin-stimulation increased IRS-1-associated p85 protein levels and PI 3-kinase activity in the LDM fraction of control but not BSO-treated cells. Thus, BSO treatment disrupts insulin-induced IRS-1 phosphorylation in the LDM fraction and the subcellular redistribution of PI 3-kinase in 3T3-L1 adipocytes.

Inhibition of NF-κB activation improves BSO-induced insulin resistance. It is widely known that one potential target of oxidative stress is the activation of transcription factor NF-κB [33]. Oxidative stress and inflammatory cytokine stimulation reportedly activate upper kinase IκB kinase (IKK) which phosphorylates serine residues of IκB. The phosphorylated IκB is then subject to degradation, leading to translocation of NF-κB to the nucleus [34]. To investigate the role of NF-κB cascade activation in BSO-induced insulin re-

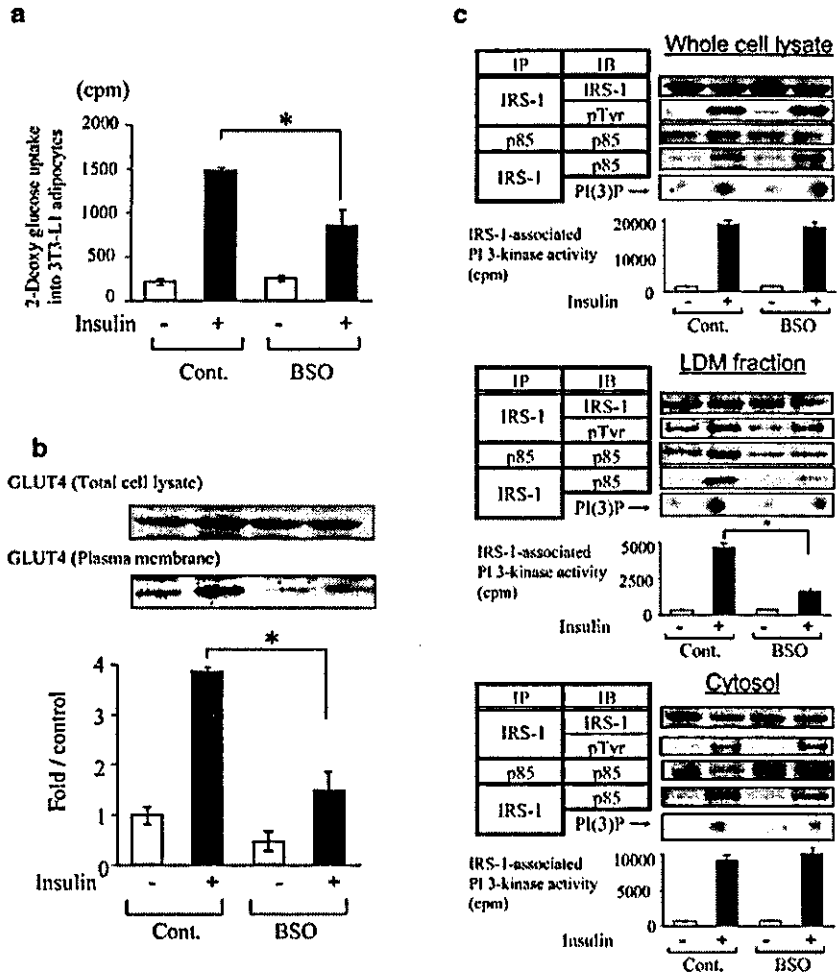

Fig. 4. Effects of BSO treatment on insulin action and insulin signalling in 3T3-L1 adipocytes. **a.** Insulin-induced 2-deoxy glucose uptake into 3T3-L1 adipocytes. 3T3-L1 adipocytes were serum-starved for 18 h, pre-incubated with or without 80 μmol/l BSO for 18 h, then incubated with or without 10^{-6} mol/l insulin for 15 min. 2-Deoxy glucose uptake was measured as described in Materials and methods. Bars depict means ± SE of results obtained independently in triplicate. * $p<0.05$ compared with the insulin-stimulated control. **b.** Recruitment of GLUT4 to the plasma membrane in 3T3-L1 adipocytes with or without BSO pretreatment. 3T3-L1 adipocytes were serum-starved for 18 h, pre-incubated with or without 80 μmol/l BSO for 18 h, then stimulated with or without 10^{-6} mol/l insulin for 15 min. Cells were fractionated as described previously [27]. The cell lysates and plasma membrane fraction were immunoblotted with anti-GLUT4 antibody. Representative immunoblots using anti-GLUT4 antibody are shown. Bars depict means ± SE of the quantitated bands of the plasma membrane fraction, independently obtained in triplicate. **c.** IRS-1 phosphorylation and IRS-1-associated PI 3-kinase in whole cell lysates (upper panels), the LDM fraction (middle panels) and the cytosol (lower panels) in 3T3-L1. 3T3-L1 adipocytes were serum-starved for 18 h, pre-incubated with or without 80 μmol/l BSO for 18 h, then stimulated with or without 10^{-6} mol/l insulin for 15 min. Subcellular fractionation was performed as described in Materials and methods. The whole cell lysates and fractions were used for immunoprecipitation, immunoblotting and PI 3-kinase assay as described previously [28]. Proteins were visualised with enhanced chemiluminescence and band intensities were quantified with a Molecular Imager GS-525. Representative immunoblots are shown in the upper and middle panels and representative spots of PI(3)P, independently obtained in triplicate, are shown in the lower panel. Bars depict means ± SE of the quantitated spots of PI(3)P, indicating IRS-1-associated PI 3-kinase activity, independently obtained in triplicate. Cont., control 3T3-L1 adipocytes; BSO, pre-treated with 80 μmol/l BSO for 18 h. * $p<0.05$ compared with the control under the insulin-stimulated condition

sistance, we overexpressed the dominant negative mutant of IκB in 3T3-L1 adipocytes using adenovirus. This mutant, characterised by the substitution of two serine phosphorylation sites to alanine, is resistant to degradation and inhibits NF-κB-induced transcription. In 3T3-L1 adipocytes, endogenous IκB was degraded by 5.8 pmol/l (equivalent to 10 ng/dl) of TNF-α or 80 μmol/l BSO pre-incubation for 18 h (Fig. 5a). However, the dominant negative IκB, overexpressed using adenovirus, was not degraded by these treat-

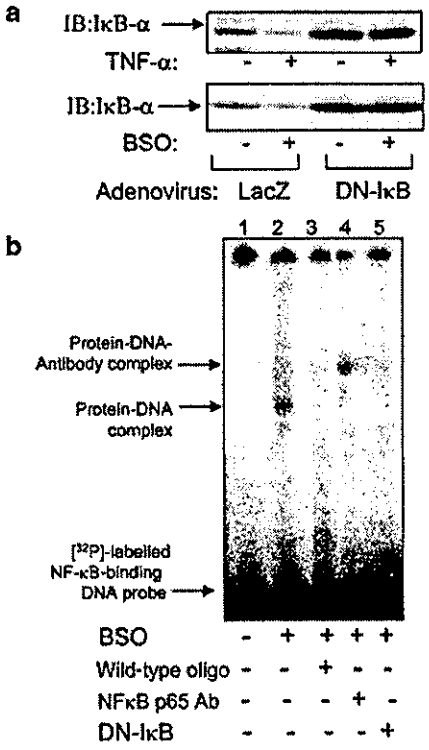

Fig. 5. Dominant negative mutant of IκB. **a.** Immunoblot of 3T3-L1 adipocytes overexpressing LacZ (control) and dominant negative mutant of I-κB adenoviruses. Representative immunoblots with anti-IκBα antibody of the cells incubated with 5.8 pmol/l (equivalent to 10 ng/ml) TNF-α and 80 μmol/l BSO for 18 h are shown in the upper and lower panels respectively. **b.** Gel mobility shift assay (GMSA). 3T3-L1 adipocytes were incubated with (lanes 2–5) or without (lane 1) 80 μmol/l BSO for 18 h. Dominant negative IκB was overexpressed in 3T3-L1 adipocytes (lane 5). Nuclear protein extracts from 3T3-L1 adipocytes were prepared as described in Materials and methods. For the GMSA, 10 μg of nuclear proteins were incubated in binding buffer with 3.5 pmol of double-stranded DNA oligonucleotide containing an NF-κB consensus binding sequence labelled with [^{32}P]-ATP using T4 polynucleotide kinase, for 30 min at 37 °C. For supershift analyses, monoclonal antibody against NF-κB p65 (NF-κB p65 Ab, lane 4) was separately pre-incubated with nuclear extracts at 4 °C for 20 min in a total volume of 16 μl of binding buffer, followed by incubation with 8 μl of ^{32}P-labelled oligonucleotide probe with and without a cold oligonucleotide probe (wild-type oligo, lane 3) at 4 °C for 20 min using a Nushift Kit (Geneka Biotechnology). Protein-DNA complexes were separated from the unbound DNA probe by electrophoresis through 5% polyacrylamide gels containing 1× Tris-glycine-EDTA buffer. The gel was dried and exposed to BAS2000 (Fujifilm, Tokyo, Japan). DN, dominant negative; IB, immunoblotting

ments (Fig. 5a). To investigate whether NF-κB binds to regulatory DNA elements, GMSA was performed using nuclear extracts of 3T3-L1 adipocytes. GMSA revealed nuclear protein extracts from BSO-treated 3T3-L1 adipocytes to contain activated NF-κB (Fig. 5b, lanes 1 and 2). The band shift was inhibited by unlabelled oligonucleotide corresponding to a DNA-binding sequence (Fig. 5b, lane 3). In BSO-treated cells, the NF-κB-oligonucleotide complex underwent a supershift in the presence of antibodies against the p65 subunit of NF-κB, indicating that binding to the oligonucleotide is NF-κB-specific (Fig. 5b, lane 4). In 3T3-L1 adipocytes overexpressing the dominant negative IκB, the band shift was also inhibited (Fig. 5b, lane 5). These results suggest that BSO treatment induces NF-κB translocation and that the dominant negative IκB blocks NF-κB pathway activation.

We next examined the effect of the dominant negative IκB on BSO-induced insulin resistance. Insulin-induced glucose uptake was decreased by BSO treatment, while dominant negative IκB overexpression reversed this decrease (Fig. 6a). Reduction of insulin-induced GLUT4 translocation by BSO administration was also reversed by overexpression of the dominant negative IκB (Fig. 6b). BSO treatment decreased insulin-induced IRS-1 phosphorylation and IRS-1-associated p85 and PI 3-kinase activity in the LDM fraction (Fig. 6c, lower panels), but not in whole cell lysates (Fig. 6c, upper panels). However, overexpression of the dominant negative IκB reversed the BSO-induced decreases in IRS-1 phosphorylation and IRS-1-associated p85 and PI 3-kinase activity in the LDM fraction. These results suggest that oxidative stress induces insulin resistance by impairing the normal subcellular distribution of PI 3-kinase, and that the NF-κB pathway is involved in this process.

Discussion

In this study we employed BSO, a glutathione synthase inhibitor, to induce oxidative stress in rats and in 3T3-L1 adipocytes. BSO specifically inhibits the first step of glutathione synthesis and decreases glutathione, an important component of the antioxidant defence system [14]. In fact, we confirmed a decreased hepatic glutathione content and an increased plasma lipid hydroperoxide level, indicating increased oxidative stress in BSO-treated rats. Body weight was lower in BSO-treated rats than in controls, which is consistent with a previous report [35]. BSO-treated rats were apparently insulin-resistant, as demonstrated by a hyperinsulinaemic-euglycaemic clamp study and glucose transport assay using isolated skeletal muscle and adipocytes. These results strongly support the hypothesis that increased oxidative stress can lead to insulin resistance in vivo. Although fasting insulin levels were not elevated in BSO-treated rats as compared with controls, we found that among well-fed animals, insulin levels were significantly higher in BSO-treated rats than in controls. Data from the euglycaemic-hyperinsulinaemic clamp study, along with the observed glucose uptake into isolated tissues and insulin levels in well-fed animals, support the

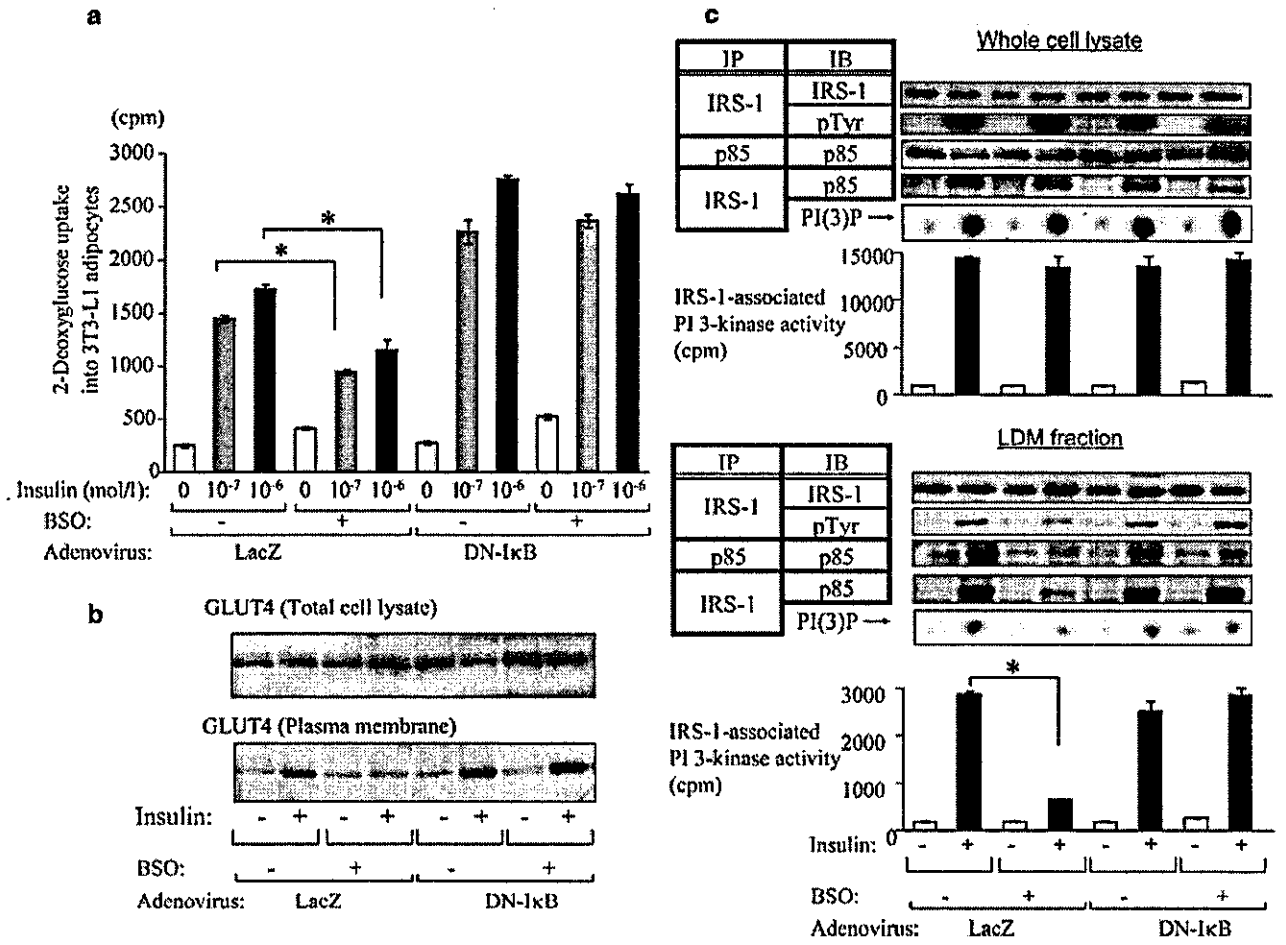

Fig. 6. Effect of dominant negative mutant of IκB on insulin action and insulin signalling in BSO-treated 3T3-L1 adipocytes. **a.** Insulin-induced 2-deoxy glucose uptake into 3T3-L1 adipocytes. Cells overexpressing LacZ (control) and the dominant negative (DN)-IκB adenovirus with or without 80 μmol/l BSO for 18 h were stimulated were stimulated with 0, 10^{-7} or 10^{-6} mol/l insulin for 15 min. Glucose uptake into 3T3-L1 adipocytes was assayed as described in Materials and methods. Bars depict means ± SE of results obtained independently in triplicate. ** $p<0.05$ compared to insulin-stimulated (10^{-7} and 10^{-6} mol/l respectively) control (non BSO-treated) cells. **b.** Recruitment of GLUT4 to the plasma membrane in 3T3-L1 adipocytes overexpressing LacZ and DN-IκB adenovirus with or without BSO pretreatment. The cell lysates and plasma membrane fraction were immunoblotted with anti-GLUT4 antibody. **c.** IRS-1 tyrosine phosphorylation, p85 protein amount and IRS-1-associated PI 3-kinase in whole cell lysates (upper panels) and the LDM fraction (lower panels) of 3T3-L1 adipocytes overexpressing LacZ and DN-IκB adenovirus with or without BSO pretreatment. 3T3-L1 adipocytes were serum-starved for 18 h, pre-incubated with or without 80 μmol/l BSO for 18 h, then stimulated with or without 10^{-6} mol/l insulin for 15 min. Representative immunoblots and representative spots of PI(3)P, independently obtained in triplicate, are shown and bars depict means ± SE of PI 3-kinase activity measured in three independent assays. * $p<0.05$ compared with insulin-stimulated control (non BSO-treated) cells. IB, immunoblotting; IP, immunoprecipitation

conclusion that BSO-treated rats are insulin-resistant. In our experiments, we did not observe the occurrence of overt diabetes with BSO administration, suggesting that this insulin resistance is relatively mild.

A previous report showed no significant difference between BSO-injected rats and controls in terms of insulin-stimulated glucose transport into skeletal muscle [15]. The results of their study contradict our present data demonstrating BSO-induced insulin resistance. We speculate that these different results are attributable to the doses of BSO administered. According to our water consumption data, intake of BSO in BSO-treated rats was approximately 3.5 mmol·kg^{-1} body weight·day^{-1} in the current study. This is a rather high dose compared with the previous report (2 mmol·kg^{-1} body weight·day^{-1}) [15]. Also, the extent of the glutathione decrease was greater in our experiment than in the previous one. In addition, because the previous study did not employ the hyperinsulinaemic-euglycaemic clamp method [15], we believe our picture of insulin resistance in BSO-treated rats to be more accurate.

Insulin-induced IRS phosphorylation and PI 3-kinase activation constitute a critical step in insulin actions such as GLUT4 translocation and glucose uptake [36]. Most insulin-resistant models have been shown

to have impaired insulin-induced PI 3-kinase activation [28, 37, 38]. However, in the BSO-treated rats used in the current study, neither insulin-induced IRS tyrosine phosphorylation nor PI 3-kinase activation in whole tissue lysates of skeletal muscle and adipose tissue were impaired, despite the presence of insulin resistance. In addition, BSO treatment markedly impaired insulin-induced glucose uptake into 3T3-L1 adipocytes and GLUT4 translocation, while insulin-induced IRS-1 tyrosine phosphorylation and IRS-1-associated PI 3-kinase activation were unchanged in whole cell lysates of BSO-treated 3T3-L1 adipocytes. A previous report showed H_2O_2 exposure of 3T3-L1 adipocytes to inhibit insulin-induced glucose uptake, while having no effects on IRS-1 phosphorylation and PI 3-kinase activation [39]. Furthermore, we previously reported chronically angiotensin-II-infused rats, in which plasma lipid hydroperoxide levels were increased, to be highly insulin-resistant, although insulin-induced IRS-1 phosphorylation and PI 3-kinase activation in skeletal muscle and adipose tissue were not impaired [12]. Thus, insulin resistance with normal insulin-induced PI 3-kinase activation in the whole cell may be a common feature in the models with increased oxidative stress.

Regarding the molecular mechanism of this type of insulin resistance, we consider it necessary to examine the possibility of abnormalities in the subcellular distribution of PI 3-kinase. This is based on several reports showing IRS-1 phosphorylation and PI 3-kinase activation specifically in the LDM fraction, though not in whole cell lysates, to be important for insulin action [30, 31]. We speculate that the insulin-induced increase in IRS-1 phosphorylation in the LDM fraction leads to recruitment of the p85 subunit for PI 3-kinase to that fraction. Previous reports have shown that H_2O_2 exposure reduces IRS-1 tyrosine phosphorylation and PI 3-kinase activation in the LDM fraction in 3T3-L1 adipocytes [39, 40]. In the current study, insulin-induced IRS-1 tyrosine phosphorylation in the LDM fraction was demonstrated to be significantly decreased in both BSO-treated rat muscle and adipose tissues and in BSO-treated 3T3-L1 cells. We showed clearly that insulin induces p85 translocation from the cytosol to the LDM fraction in rat muscle, adipose tissue and 3T3-L1 cells and that BSO treatment disrupts this process. Taking our results and those of previous reports together, we consider this disruption of the normal subcellular redistribution of PI 3-kinase to be one of the important mechanisms underlying oxidative-stress-induced insulin resistance.

The activation of transcription factor NF-κB has been shown to be a target of oxidative stress [33]. For example, direct exposure to oxidants such as H_2O_2 activates NF-κB [41], while NF-κB activation can be inhibited by addition of antioxidants such as a vitamin E derivative [42] and lipoic acid [43]. To clarify the contribution of NF-κB cascade activation to oxidative-stress-induced insulin resistance, we utilised the dominant negative IκB. This mutant is a degradation-resistant form of IκB that prevents NF-κB from translocating into the nucleus and is widely used to block cytokine-induced NF-κB activation [44]. Indeed, we confirmed that this mutant is not degraded by TNF-α and that BSO stimulation blocks NF-κB from translocating into the nucleus. Blocking the NF-κB cascade by overexpressing dominant negative IκB had a preventive effect against the decrease in insulin-induced glucose uptake and GLUT4 translocation caused by BSO treatment in 3T3-L1 adipocytes. We observed higher glucose uptake in dominant negative IκB-overexpressing cells than in LacZ control cells. We suggest a possible explanation: dominant negative IκB inhibits the effects of a small amount of inflammatory cytokines secreted by adipocytes. In addition, BSO-induced decreases in IRS-1 tyrosine phosphorylation in the LDM fraction and recruitment of PI 3-kinase to that fraction were also normalised. These results suggest that NF-κB activation is involved in the impaired subcellular redistribution of PI 3-kinase and the insulin resistance induced by BSO treatment.

The precise mechanism linking NF-κB activation and abnormal subcellular redistribution of PI 3-kinase remains unclear. One possible mechanism of inhibited insulin signalling involves NF-κB-activated transcription of inflammatory cytokines such as TNF-α and interleukin-6. NF-κB plays an important role in regulating inflammatory responses [45, 46] and activation of NF-κB may induce inappropriate inflammatory responses, possibly disrupting insulin signalling. Alternatively, PI 3-kinase activation is reportedly necessary for NF-κB activation [47, 48]. Aberrant NF-κB activation may disrupt the PI 3-kinase pathway via a negative feedback mechanism. An anti-inflammatory agent, salicylate, which stabilises IκB via inhibition of IKK and suppression of NF-κB activation, was shown to restore lipid-induced insulin resistance [49, 50]. Because IKK reportedly induces serine phosphorylation of IRS-1, it is possible that BSO activates IKK, resulting in down-regulation of IRS-1 tyrosine phosphorylation in the LDM fraction and impairment of PI 3-kinase recruitment to the LDM fraction.

In summary, our results suggest that oxidative stress induces insulin resistance by impairing insulin-induced IRS-1 phosphorylation in the LDM fraction and subcellular redistribution of PI 3-kinase, and that NF-κB activation is involved in this process. Our present study provides evidence that the NF-κB pathway plays a role in the pathogenesis of oxidative-stress-induced insulin resistance. Judging from our results and those of previous studies, strategies designed to limit inappropriate activation of NF-κB may be an effective approach to treating insulin resistance.

Acknowledgements. The dominant negative mutant of IκB was kindly provided by Dr Richard Gaynor (University of Texas Southwestern Medical Center at Dallas, Tex., USA). The authors are indebted to Naomasa Kakiya of the University of Tokyo for assistance in various areas of this study.

References

1. Betteridge DJ (2000) What is oxidative stress? Metabolism 49 [Suppl 1]:3–8
2. Reaven GM, Lithell H, Landsberg L (1996) Hypertension and associated metabolic abnormalities—the role of insulin resistance and the sympathoadrenal system. N Engl J Med 334:374–381
3. Tuck ML (1990) Metabolic considerations in hypertension. Am J Hypertens 3:355S–365S
4. Baynes JW (1991) Role of oxidative stress in development of complications in diabetes. Diabetes 40:405–412
5. Paolisso G, D'Amore A, Volpe C et al. (1994) Evidence for a relationship between oxidative stress and insulin action in non-insulin-dependent (type II) diabetic patients. Metabolism 43:1426–1429
6. Jones AF, Winkles JW, Jennings PE et al. (1988) Serum antioxidant activity in diabetes mellitus. Diabetes Res 7:89–92
7. Paolisso G, Di Maro G, Pizza G et al. (1992) Plasma GSH/GSSG affects glucose homeostasis in healthy subjects and non-insulin-dependent diabetics. Am J Physiol 263:E435–E440
8. Paolisso G, Balbi V, Volpe C et al. (1995) Metabolic benefits deriving from chronic vitamin C supplementation in aged non-insulin dependent diabetics. J Am Coll Nutr 14:387–392
9. Paolisso G, Di Maro G, Galzerano D et al. (1994) Pharmacological doses of vitamin E and insulin action in elderly subjects. Am J Clin Nutr 59:1291–1296
10. Rajagopalan S, Kurz S, Munzel T et al. (1996) Angiotensin II-mediated hypertension in the rat increases vascular superoxide production via membrane NADH/NADPH oxidase activation. Contribution to alterations of vasomotor tone. J Clin Invest 97:1916–1923
11. Schnackenberg CG, Wilcox CS (1999) Two-week administration of tempol attenuates both hypertension and renal excretion of 8-Iso prostaglandin f2alpha. Hypertension 33:424–428
12. Ogihara T, Asano T, Ando K et al. (2002) Angiotensin II-induced insulin resistance is associated with enhanced insulin signalling. Hypertension 40:872–879
13. Shimosawa T, Ogihara T, Matsui H et al. (2003) Deficiency of adrenomedullin induces insulin resistance by increasing oxidative stress. Hypertension 41:1080–1085
14. Meister A (1983) Selective modification of glutathione metabolism. Science 220:472–477
15. Khamaisi M, Kavel O, Rosenstock M et al. (2000) Effect of inhibition of glutathione synthesis on insulin action: in vivo and in vitro studies using buthionine sulfoximine. Biochem J 349:579–586
16. Vaziri ND, Wang XQ, Oveisi F, Rad B (2000) Induction of oxidative stress by glutathione depletion causes severe hypertension in normal rats. Hypertension 36:142–146
17. Ogihara T, Asano T, Ando K et al. (2001) Insulin resistance with enhanced insulin signalling in high-salt diet-fed rats. Diabetes 50:573–583
18. Yamamoto Y (1994) Chemiluminescence-based high-performance liquid chromatography assay of lipid hydroperoxides. Methods Enzymol 233:319–324
19. Anderson ME (1985) Determination of glutathione and glutathione disulfide in biological samples. Methods Enzymol 113:548–555
20. James DE, Burleigh KM, Kraegen EW (1986) In vivo glucose metabolism in individual tissues of the rat. Interaction between epinephrine and insulin. J Biol Chem 261:6366–6374
21. Hansen P, Gulve EA, Holloszy JO (1994) Suitability of 2-deoxyglucose for in vitro measurement of glucose transport activity in skeletal muscle. J Appl Physiol 76:979–985
22. Rodbell M (1964) Metabolism of isolated fat cells. I. Effects of hormones on glucose metabolism and lipolysis. J Biol Chem 239:375–380
23. Olefsky JM (1975) Effect of dexamethasone on insulin binding, glucose transport, and glucose oxidation of isolated rat adipocytes. J Clin Invest 56:1499–1508
24. Fujishiro M, Gotoh Y, Katagiri H et al. (2001) MKK6/3 and p38 MAPK pathway activation is not necessary for insulin-induced glucose uptake but regulates glucose transporter expression. J Biol Chem 276:19800–19806
25. Katagiri H, Asano T, Ishihara H et al. (1996) Overexpression of catalytic subunit p110alpha of phosphatidylinositol 3-kinase increases glucose transport activity with translocation of glucose transporters in 3T3-L1 adipocytes. J Biol Chem 271:16987–16990
26. Asano T, Kanda A, Katagiri H et al. (2000) p110beta is up-regulated during differentiation of 3T3-L1 cells and contributes to the highly insulin-responsive glucose transport activity. J Biol Chem 275:17671–17676
27. Satoh S, Nishimura H, Clark AE et al. (1993) Use of bismannose photolabel to elucidate insulin-regulated GLUT4 subcellular trafficking kinetics in rat adipose cells. Evidence that exocytosis is a critical site of hormone action. J Biol Chem 268:17820–17829
28. Anai M, Funaki M, Ogihara T et al. (1998) Altered expression levels and impaired steps in the pathway to phosphatidylinositol 3-kinase activation via insulin receptor substrates 1 and 2 in Zucker fatty rats. Diabetes 47:13–23
29. Sakoda H, Ogihara T, Anai M et al. (1999) No correlation of plasma cell 1 overexpression with insulin resistance in diabetic rats and 3T3-L1 adipocytes. Diabetes 48:1365–1371
30. Anai M, Ono H, Funaki M et al. (1998) Different subcellular distribution and regulation of expression of insulin receptor substrate (IRS)-3 from those of IRS-1 and IRS-2. J Biol Chem 273:29686–29692
31. Kriauciunas KM, Myers MG Jr, Kahn CR (2000) Cellular compartmentalization in insulin action: altered signaling by a lipid-modified IRS-1. Mol Cell Biol 20:6849–6859
32. Lu B, Ennis D, Lai R et al. (2001) Enhanced sensitivity of insulin-resistant adipocytes to vanadate is associated with oxidative stress and decreased reduction of vanadate (+5) to vanadyl (+4). J Biol Chem 276:35589–35598
33. Schreck R, Albermann K, Baeuerle PA (1992) Nuclear factor kappa B: an oxidative stress-responsive transcription factor of eukaryotic cells (a review). Free Radic Res Commun 17:221–237
34. Siebenlist U, Franzoso G, Brown K (1994) Structure, regulation and function of NF-kappa B. Annu Rev Cell Biol 10:405–455
35. Leeuwenburgh C, Ji LL (1995) Glutathione depletion in rested and exercised mice: biochemical consequence and adaptation. Arch Biochem Biophys 316:941–949
36. Czech MP (1995) Molecular actions of insulin on glucose transport. Annu Rev Nutr 15:441–471

37. Saad MJ, Folli F, Kahn JA, Kahn CR (1993) Modulation of insulin receptor, insulin receptor substrate-1, and phosphatidylinositol 3-kinase in liver and muscle of dexamethasone-treated rats. J Clin Invest 92:2065–2072
38. Cusi K, Maezono K, Osman A et al. (2000) Insulin resistance differentially affects the PI 3-kinase- and MAP kinase-mediated signalling in human muscle. J Clin Invest 105:311–320
39. Rudich A, Tirosh A, Potashnik R, Hemi R, Kanety H, Bashan N (1998) Prolonged oxidative stress impairs insulin-induced GLUT4 translocation in 3T3-L1 adipocytes. Diabetes 47:1562–1569
40. Tirosh A, Potashnik R, Bashan N, Rudich A (1999) Oxidative stress disrupts insulin-induced cellular redistribution of insulin receptor substrate-1 and phosphatidylinositol 3-kinase in 3T3-L1 adipocytes. A putative cellular mechanism for impaired protein kinase B activation and GLUT4 translocation. J Biol Chem 274:10595–10602
41. Schreck R, Rieber P, Baeuerle PA (1991) Reactive oxygen intermediates as apparently widely used messengers in the activation of the NF-kappa B transcription factor and HIV-1. EMBO J 10:2247–2258
42. Suzuki YJ, Packer L (1993) Inhibition of NF-kappa B activation by vitamin E derivatives. Biochem Biophys Res Commun 193:277–283
43. Sen CK, Packer L (1996) Antioxidant and redox regulation of gene transcription. FASEB J 10:709–720
44. Yamamoto Y, Gaynor RB (2001) Therapeutic potential of inhibition of the NF-kappaB pathway in the treatment of inflammation and cancer. J Clin Invest 107:135–142
45. Baeuerle PA, Henkel T (1994) Function and activation of NF-kappa B in the immune system. Annu Rev Immunol 12:141–179
46. Barnes PJ, Karin M (1997) Nuclear factor-kappaB: a pivotal transcription factor in chronic inflammatory diseases. N Engl J Med 336:1066–1071
47. Sizemore N, Leung S, Stark GR (1999) Activation of phosphatidylinositol 3-kinase in response to interleukin-1 leads to phosphorylation and activation of the NF-kappaB p65/RelA subunit. Mol Cell Biol 19:4798–4805
48. Reddy SA, Huang JH, Liao WS (2000) Phosphatidylinositol 3-kinase as a mediator of TNF-induced NF-kappa B activation. J Immunol 164:1355–1363
49. Kim JK, Kim YJ, Fillmore JJ et al. (2001) Prevention of fat-induced insulin resistance by salicylate. J Clin Invest 108:437–446
50. Yuan M, Konstantopoulos N, Lee J et al. (2001) Reversal of obesity- and diet-induced insulin resistance with salicylates or targeted disruption of Ikkbeta. Science 293:1673–1677

FEBS 28636 FEBS Letters 571 (2004) 187–191

Feeding induces expression of heat shock proteins that reduce oxidative stress

Kensaku Katsuki[a,b], Mitsuaki Fujimoto[a], Xiu-Ying Zhang[a], Hanae Izu[a], Eiichi Takaki[a], Yukio Tanizawa[b], Sachiye Inouye[a], Akira Nakai[a,*]

[a]*Department of Biochemistry and Molecular Biology, Yamaguchi University School of Medicine, Minami-Kogushi 1-1-1, Ube 775-8505, Japan*
[b]*Third Department of Internal medicine, Yamaguchi University School of Medicine, Minami-Kogushi 1-1-1, Ube 775-8505, Japan*

Received 8 June 2004; revised 22 June 2004; accepted 22 June 2004

Available online 14 July 2004

Edited by Barry Halliwell

Abstract Heat shock proteins (Hsps) are induced in response to various kinds of environmental and physiological stresses. However, it is unclear whether Hsps play roles in protecting cells in the digestive organs against xenobiotic chemicals. Here, we found that feeding induces expression of a set of Hsps specifically in the mouse liver and intestine by activating heat shock transcription factor 1 (HSF1). In the liver, HSF1 is required to suppress toxic effects of electrophiles, which are xenobiotic chemicals causing oxidative stress. We found that overexpression of Hsp27, which elevates cellular glutathione level, promotes survival of culture cells exposed to electrophiles. These results suggest a novel mechanism of cell protection against xenobiotic chemicals in the food.

Keywords: Electrophile; Glutathione; Heat shock protein; Heat shock transcription factor; Liver; Oxidative stress

1. Introduction

Heat shock response, which is characterized by the induction of a set of heat shock proteins (Hsps), is a fundamental response in all organisms to protect themselves from environmental stresses such as heat, oxidative stress, ischemia, inflamation and exposure to toxic chemicals [1]. This response is regulated mainly at a transcription level by heat shock transcription factor 1 (HSF1) in mammals [2]. There are many Hsps belonging to diverse families and Hsps act coordinately to assist the folding of cellular proteins [3]. Hsps also bind to denatured proteins, prevent misaggregation and facilitate renaturation. In addition to the "foldase activity", each Hsp has a unique role. For example, Hsp27 reduces oxidative stress by raising the pool of reduced glutathione (GSH) in the cells [4].

In addition to environmental stresses, heat shock response is induced in response to physiological stresses such as exercise [5,6] and restraint stress [7,8]. Here, we found that feeding induces expression of Hsps selectively in the liver and intestine among digestive organs. Digested elements such as oligosaccharides, proteins, lipids and nucleic acids are adsorbed mostly in the intestine, and blood containing these elements is directly transported to the liver through the portal vein. To protect themselves from xenobiotic chemicals such as electrophiles in the food, detoxifying enzymes are rich in the liver [9,10]. We found that electrophiles induce heat shock response in HeLa and Jurkat cells, probably by causing oxidative stress. Furthermore, induction of at least Hsp27 reduced toxic effects of electrophiles on culture cells.

2. Materials and methods

2.1. Animals, food and injection of DEM

Mice of ICR background were maintained at 24 °C with light on from 8 to 20 h. 6-week-old mice had free access to water and diet (bleeding grade F-1, Oriental Yeast Co., Ltd, Tokyo, Japan). Food deprivation was performed for 48 h and then the same diet was fed for indicated periods. Digestive organs were immediately dissected and stored at −80 °C until use. To examine the expression of Hsps in the absence of HSF1, HSF1-null mice were used [11]. Diethyl maleate (DEM) (Wako, Osaka, Japan) prepared in sesame oil (5.3 mmol of DEM/kg of body weight) was injected intraperitoneally and serum alanine aminotransferase (ALT) levels were measured (SRL Co., Tokyo, Japan). All experimental protocols were reviewed by the Committee for Ethics on Animal Experiments of Yamaguchi University School of Medicine.

2.2. Western blot analysis, Gel shift assay and Northern blot analysis

Tissues were dissected, immediately frozen and stored at −80 °C until use. The extracts were prepared with NP-40 lysis buffer [150 mM NaCl, 1.0% Nonidet P-40, 50 mM Tris (pH 8.0), 1 mM phenylmethylsulfonyl fluoride, 1 μg/ml leupeptin and 1 μg/ml pepstatin]. HeLa cell extracts were also prepared with NP-40 lysis buffer. Western blot analysis was performed as described previously [12] using mouse monoclonal IgG for Hsp70 (W27, Santa Cruiz), and antiserum for human Hsp70 (Fujimoto, unpublished), rat Hsp27 (a kind gift from K. Kato), and human GST-pi (Novocastra Lab. Ltd., UK). To detect Hsp90, we generated a specific antiserum. Recombinant human Hsp90α (amino acids 333–732) fused to glutathione-*S*-transferase was immunized in rabbits in a TiterMax (CrtRx Co., Georgia) water-in-oil emulsion. The levels of Hsp70 protein in various tissues were estimated by using NIH image.

To perform gel shift assay, mice were systematically anesthetized with ketamine (16 mg/kg, i.p.) and xylazine (16 mg/kg, i.p.) and perfused with phosphate-buffered saline. Whole tissue extracts were prepared from the liver, and gel shift assay and supershift experiments were performed as described previously [12].

Northern blot analysis was performed essentially as described previously [13].

2.3. Cells and the treatment with reagents

HeLa cells were maintained at 37 °C in 5% CO_2 in Dulbecco's modified Eagle's medium containing 10% fetal calf serum at 37 °C in

* Corresponding author. Fax: +81-836-22-2315.
E-mail address: anakai@yamaguchi-u.ac.jp (A. Nakai).

0014-5793/$22.00 © 2004 Published by Elsevier B.V. on behalf of the Federation of European Biochemical Societies.
doi:10.1016/j.febslet.2004.06.087

5% CO_2. HeLa cells stably expressing mouse Hsp27 were described previously [14]. To prepare HeLa cells expressing human GST-pi (pcDNA3.1/GST-pi), GST-pi cDNA [15] was cloned by RT-PCR and was inserted into pcDNA3.1(+) (Invitrogen). The DNA was transfected into HeLa cells by a calcium-phosphate method and cells grown in the presence of 1.5 mg/ml of G418 were selected as described previously [14]. Jurkat cells were maintained in RPMI containing 10% fetal calf serum. To block de novo synthesis of glutathione, cells were treated with 0.1 mM L-buthionine-(*S*,*R*)-sulfoximine (BSO) (stock, 100 mM in H_2O) (Sigma, St. Louis, MO) until 48 h. Cells were also treated with electrophile, 1-chloro-2,4-dinitrobenzene (CDNB) (stock, 10 mM in 100% ethanol) or DEM (stock, 10 mM in 100% ethanol) at a concentration of 10 to 40 μM for 8 h.

To examine cell survival, HeLa cells were treated with CDNB for 24 h and were replated in dishes containing normal medium for 10 days. Cells were fixed in 70% ethanol for 30 min and then stained with Giemsa's stain solution (Muto Pure Chemicals, Tokyo, Japan). Colonies counted, and means and S.D. were calculated from three independent experiments.

2.4. Determination of glutathione levels

Total cellular glutathione concentrations (reduced plus oxidized forms) were measured as described previously [16,17] and showed as nanomoles per 1×10^6 cells.

3. Results

3.1. Feeding induces heat shock response specifically in the liver and intestine

To reveal whether feeding induces expression of Hsps in various tissues, mice starved for 48 h were fed for 3 h and expression of Hsp70 protein was determined. We found that Hsp70 expression was induced in the liver and the intestine after feeding, but was not induced in the colon, stomach, brain and muscle (Fig. 1A). As the liver is important for detoxifying chemicals, we further analyzed the response in the liver. Inductions of proteins and mRNAs of Hsp70 and Hsp90 were observed even 1 h after feeding, and induction of Hsp27 protein was particularly strong although it was detected firstly at 6 h after feeding (Fig. 1B). Induction of Hsp70 was low probably due to unique regulation of Hsp70 in the liver [18].

3.2. HSF1 plays roles in suppressing toxic effects of electrophiles in the liver

We next examined HSF1 activation in the liver. Weak, but distinct HSE-binding activity of HSF was induced 1 h after feeding in the liver and then the activity attenuated (Fig. 2A). Supershift experiment using specific antiserum showed that the HSE-binding activity was composed of HSF1 (data not shown). We next examined the induction of Hsp90, Hsp70 and Hsp27 expression after feeding in HSF1-null mice. We observed no induction of Hsps in HSF1-null mice (Fig. 2B), indicating that HSF1 is required for the feeding-induced induction of Hsps in the liver.

To examine whether HSF1 plays roles in rendering toxic effects of xenobiotic chemicals in the liver, an electrophilic reagent DEM was injected intraperitoneally. We determined toxic effects of DEM on liver cells by estimating levels of serum ALT that is released from damaged liver cells. We found that serum ALT levels did not increase in both wild-type starved and feeding mice injected with 5.3 mmol of DEM/kg of body weight (41.7 and 30.7 IU/L, respectively), but increased in DEM-injected starved HSF1-null mice (69.7 IU/L) (Fig. 2C). Furthermore, ALT level in DEM-injected feeding HSF1-null mice (174.3 IU/L) was much higher than that in starved mice.

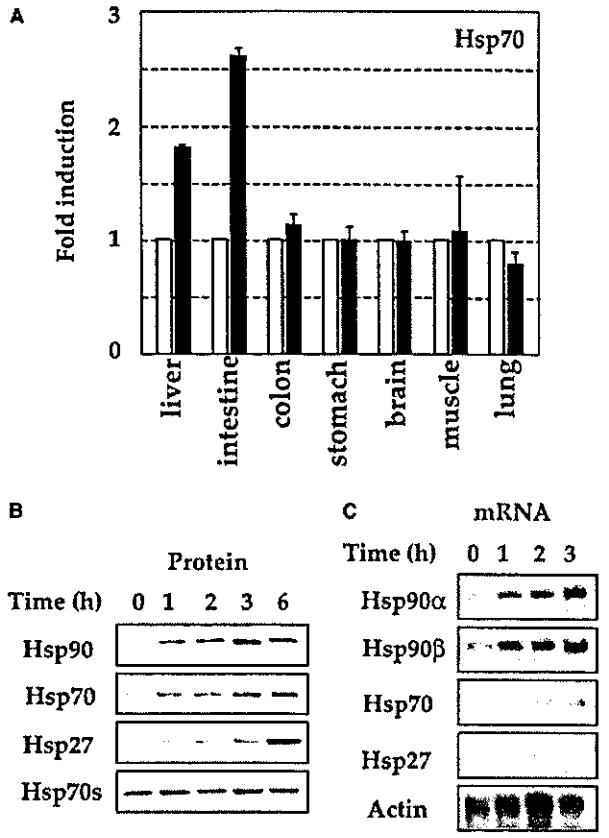

Fig. 1. Feeding induces heat shock response in the liver and intestine. (A) 6-week-old mice were starved for 48 h (open bars) and then fed for 3 h (closed bars). Expression levels of Hsp70 in various tissues were determined by Western blot analysis and were normalized by expression levels of β-actin. Means and S.D. of fold inductions from three independent experiments are shown. (B) Starved mice for 48 h (0) were fed for 1, 2, 3 and 6 h. Expression levels of Hsps in the liver were determined by Western blot analysis using each specific antibody and antibody recognizing Hsp70 and Hsc70 (Hsp70s). Representative data are shown from three experiments. (C) Starved mice for 48 h (0) were fed for 1, 2 and 3 h. Expression levels of Hsps in the liver were determined by Northern blot analysis using each specific cDNA probes. Representative data are shown from three experiments.

These results suggest that HSF1 plays roles in suppressing toxic effects of electrophiles in the liver.

3.3. Electrophiles induce heat shock response

As we found a little induction of Hsps in the liver by injection with 5.3 mmol of DEM/kg of body weight (data not shown), we analyzed the response of cultured HeLa and Jurkat cells to electrophiles. We found that electrophiles, both DEM and CDNB, induced activation of HSF1 and expression of Hsp70 (Fig. 3A and B, data not shown). BSO reduces de novo synthesis of cellular glutathione level (Fig. 3C), and Hsp90, Hsp70, Hsp40 and Hsp27 were induced at lower concentrations of CDNB when the level of glutathione was reduced (Fig. 3D). These results suggest that electrophiles cause oxidative stress that induces heat shock response.

3.4. Hsp27 reduces toxic effects of electrophiles on culture cells

Because Hsp27 expression is markedly induced by the feeding and was too low to be detected in HSF1-null liver

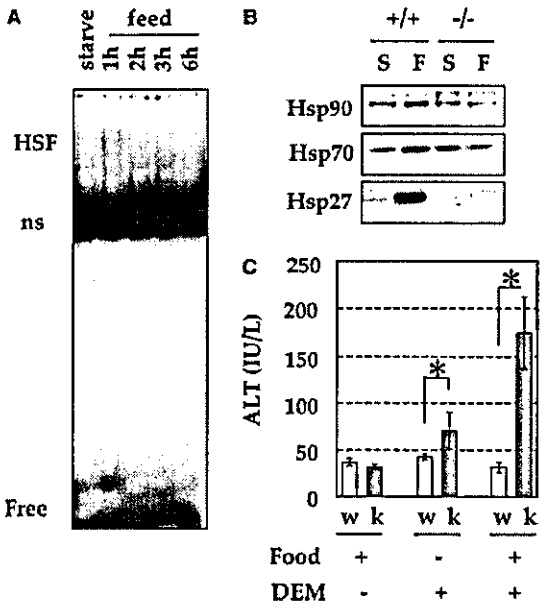

Fig. 2. HSF1 is required for feeding-induced induction of Hsps and protection from an electrophile in the liver. (A) Starved mice for 48 h (starvation) were fed for 1, 2, 3 and 6 h. HSE-binding activities in the liver extracts were determined by gel shift assay using a ^{32}P-labelled HSE-oligonucleotide. HSF, complexes of HSF and HSE-probe; Free, free oligonucleotide; ns, non-specific binding. (B) 6-week-old wild-type (+/+) and HSF1-null (−/−) mice were starved for 48 h (S), and then fed for 6 h (F). Expression levels of Hsp90, Hsp70 and Hsp27 were determined by Western blot analysis. (C) In a starved mouse group (food −), wild-type (w) and HSF1-null (k) mice were starved for 42 h and were injected with DEM. At 6 h after the injection, mice were fed for 24 h and serum ALT levels were determined. In a fed mouse group (food +), mice were starved for 42 h. After they were fed for 6 h, mice were injected with DEM. Serum ALT levels were determined 24 h after the injection. Serum ATL levels were also determined without DEM injection (DEM −). Means and S.D. from three experiments are shown. Stars indicate $P < 0.05$. Representative data are shown from at least three experiments.

(Fig. 2B), we examined whether overexpression of Hsp27 into HeLa cells [14] reduces toxic effects caused by electrophiles. As a control, we also generate HeLa cells overexpressing GST-pi (GST/HeLa), which promotes conjugation of glutathione to chemicals. Glutathione level was increased twofold in Hsp27/HeLa cells. Induction of Hsp70 was observed in response to 40 μM of CDNB in HeLa and GST/HeLa cells, whereas we detect no induction of Hsp70 in Hsp27/HeLa cells even in the presence of 40 μM of CDNB. Overexpression of Hsp27 prevented the induction of HSE-binding activity (data not shown). Furthermore, we found that survival of cells exposed to CDNB was significantly promoted in the presence of Hsp27 (Fig. 4D). These results indicate that induction of Hsp27 reduces toxic effects of electrophiles on culture cells.

4. Discussion

Digestive organs are frequently exposed to xenobiotic chemicals in food. These chemicals are adsorbed in the small intestine and then transported into the liver, where xenobiotic chemicals are mainly detoxified [9,10]. Therefore, it is interesting to show that feeding induces the heat shock response only in the liver and small intestine among digestive organs. Previously, it was reported that feeding induces molecular chaperones located in the endoplasmic reticulum in the liver [19,20]. However, this is the first demonstration that feeding induces a set of cytoplasmic Hsps. Furthermore, we found that feeding induces heat shock response by activating HSF1, which is also activated by heat shock [2]. Although heat shock-induced activation of HSF1 is triggered by denaturation of cellular proteins, it is unlikely that normal food induces denaturation of proteins. HSF1 may be activated through an unknown pathway to cope with unexpected toxicants such as electrophilic agents in the food.

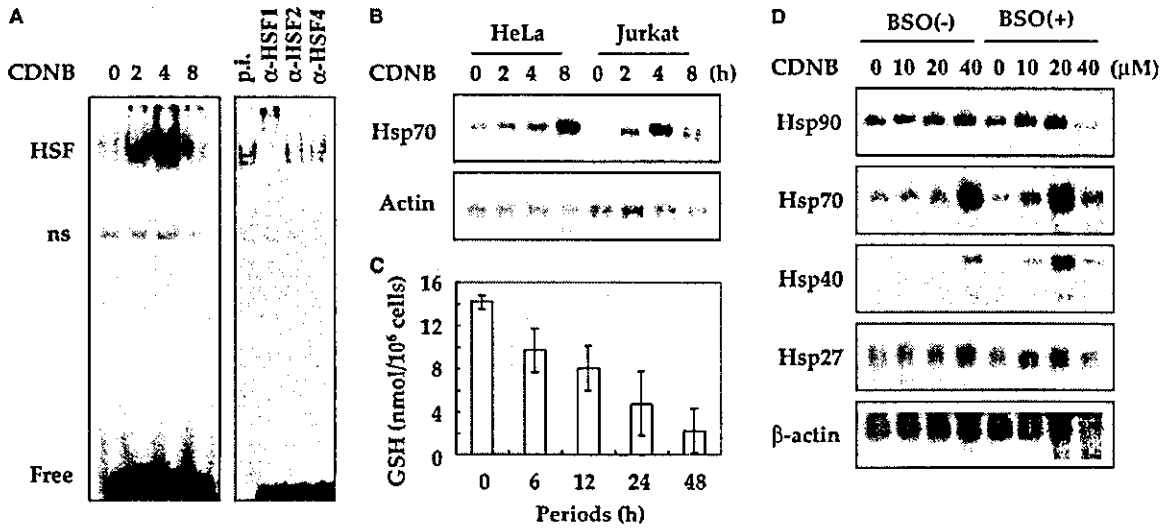

Fig. 3. CDNB induces heat shock response. (A) HeLa cells were treated with 40 μM of CDNB for indicated periods and gel shift assay was performed using a ^{32}P-labelled HSE-oligonucleotide (left). A supershift experiment of extract prepared from cells treated with CDNB for 4 h using preimmune serum (p.i.) or each specific antiserum. (B) HeLa and Jurkat cells were treated with CDNB as described in A. Northern blot analysis was performed using a cDNA probe specific for Hsp70 or β-actin. (C) HeLa cells were treated with 0.1 mM BSO for indicated periods. Levels of GSH were measured. Means and S.D. of three independent experiments are shown. (D) HeLa cells were treated with 0.1 mM BSO for 40 h and further incubated in the presence of 0, 10, 20 or 40 mM CDNB for 8 h. Total RNAs were isolated and Northern blot analysis was performed.

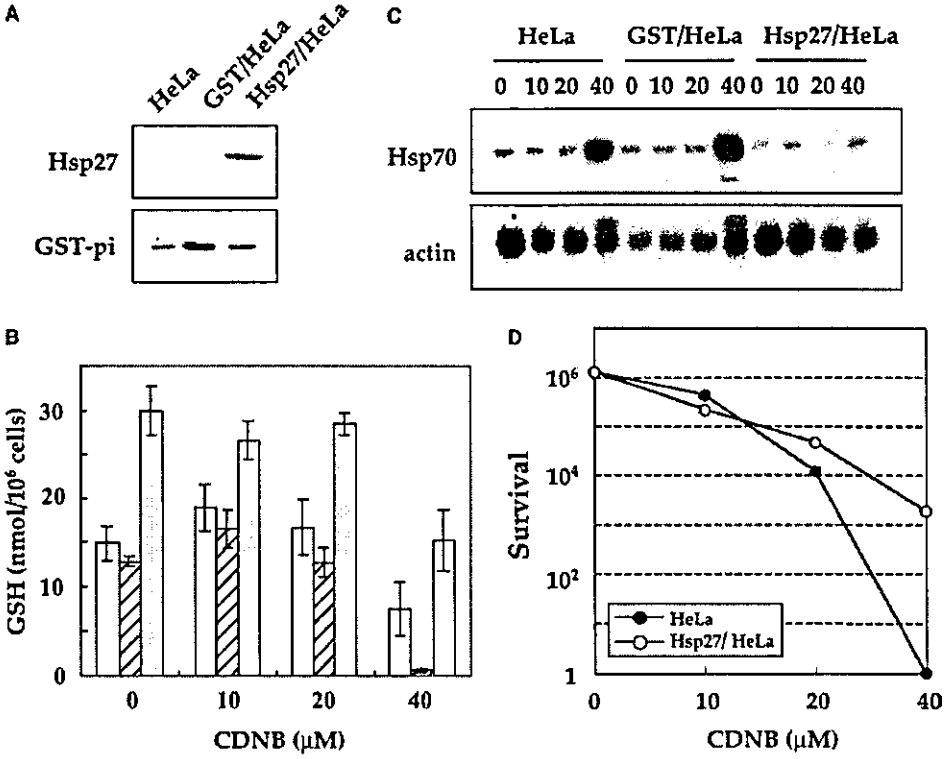

Fig. 4. Hsp27 reduces oxidative stress caused by CDNB. (A) HeLa cells were stably transfected with GST-pi expression vector or Hsp25 expression vector. Levels of Hsp25 and GST-pi were determined by Western blot analysis. (B) Cells were treated with 0, 10, 20 and 40 μM of CDNB for 8 h, and levels of GSH were measured. Means and S.D. of three independent experiments are shown. Open bar, HeLa; hatched bar, GST/HeLa; gray bar, Hsp27/HeLa. (C) Cells treated as described in B were harvested, and total RNAs were isolated from the cells and Northern blot analysis was performed. Representative data are shown from three experiments. (D) HeLa and Hsp27/HeLa cells were incubated in the presence of 0, 10, 20 or 40 μM CDNB for 24 h, and replated in dishes containing normal medium for 10 days. Means of three independent experiments of cell survivals are shown. S.D. are too small to be shown.

Electrophiles cause oxidative stress with rapid reduction of cellular glutathione level [21]. To cope with electrophiles and oxidants, cells induce phase 2 enzymes such as glutathione *S*-transferase and NAD(P)H:quinone oxidoreductase [22,23] by activating Nrf2 transcription factor [24,25]. Induction of these enzymes is accompanied by elevation of intracellular glutathione levels [26,27]. In addition to Nrf2 activation, we showed here that HSF1 is activated by electrophiles. This result might be expected because diamide and menadione, which induce oxidation of protein thiols by rapidly forming GSSG with subsequent GSH depletion, activate HSF1 [28,29]. The oxidation of protein thiols may cause denaturation of proteins, resulting in the formation of a state with similar properties to the thermally denatured state [30]. Here, we directly showed that overexpression of Hsp27 reduces toxic effects on cells, probably by increasing cellular GSH level. Because Hsp27 is a major inducible protein after feeding, it may play significant roles in suppressing toxic effects of xenobiotic chemicals in food.

Acknowledgements: We are grateful to Dr. M. Parmely for a protocol for DEM injection into mice. This work was supported in part by Grants-in-Aid for Scientific Research (B) (C), and on Priority Area-Cell Cycle, Life of proteins, and Cancer, from the Ministry of Education, Culture, Sports, Science and Technology, Japan, the Naitoh Foundation, and the Mochida Foundation.

References

[1] Lindquist, S. and Craig, E.A. (1988) Annu. Rev. Genet. 22, 631–677.
[2] Morimoto, R.I. (1998) Genes Dev. 12, 3788–3796.
[3] Bukau, B. and Horwich, A.L. (1998) Cell 92, 351–366.
[4] Mehlen, P., Kretz-Remy, C., Preville, X. and Arrigo, A.P. (1996) EMBO J. 15, 2695–2706.
[5] Locke, M., Noble, E.G. and Atkinson, B.G. (1990) Am. J. Physiol. 258, C723–C729.
[6] Salo, D.C., Donovan, C.M. and Davies, K.J. (1991) Free Radic. Biol. Med. 11, 239–246.
[7] Blake, M.J., Udelsman, R., Feulner, G.J., Norton, D.D. and Holbrook, N.J. (1991) Proc. Natl. Acad. Sci. USA 88, 9873–9877.
[8] Udelsman, R., Blake, M.J., Stagg, C.A., Li, D.G., Putney, D.J. and Holbrook, N.J. (1993) J. Clin. Invest. 91, 465–473.
[9] Zucker, S.D. and Gollan, J.L. (1995) in: Physiology of the Liver (Haubrich, W.S., Schaffner, F. and Berk, J.E., Eds.) Gastroenterology, Vol. 3, pp. 1858–1905, W.B. Saunders Company, Pennsylvania.
[10] Jakoby, W.B. and Ziegler, D.M. (1990) J. Biol. Chem. 265, 20715–20718.
[11] Inouye, S., Katsuki, K., Izu, H., Fujimoto, M., Sugahara, K., Yamada, S., Shinkai, Y., Oka, Y., Katoh, Y. and Nakai, A. (2003) Mol. Cell. Biol. 23, 5882–5895.
[12] Nakai, A., Kawazoe, Y., Tanabe, M., Nagata, K. and Morimoto, R.I. (1995) Mol. Cell. Biol. 15, 5168–5178.
[13] Izu, H., Inouye, S., Fujimoto, M., Shiraishi, K., Naito, K. and Nakai, A. (2004) Biol. Reprod. 70, 18–24.

[14] Katoh, Y., Fujimoto, M., Nakamura, K., Inouye, S., Sugahara, K., Izu, H. and Nakai, A. (2004) FEBS Lett. 565, 28–32.
[15] Mannervik, B., Alin, P., Guthenberg, C., Jensson, H., Tahir, M.K., Warholm, M. and Jornvall, H. (1985) Proc. Natl. Acad. Sci. USA 82, 7202–7206.
[16] Wang, F., Wang, L.Y., Wright, D. and Parmely, M.J. (1999) Infect. Immun. 67, 5409–5416.
[17] Parmely, M.J., Wang, F. and Wright, D. (2001) Infect. Immun. 69, 2621–2629.
[18] Blake, M.J., Gershon, D., Fargnoli, J. and Holbrook, N.J. (1990) J. Biol. Chem. 265, 15275–15279.
[19] Dhahbi, J.M., Mote, P.L., Tillman, J.B., Walford, R.L. and Spindler, S.R. (1997) J. Nutr. 127, 1758–1764.
[20] Dhahbi, J.M., Cao, S.X., Tillman, J.B., Mote, P.L., Madore, M., Walford and R.L., Spindler (2001) Biochem. Biophys. Res. Commun. 284, 335–339.
[21] Deneke, S.M. and Fanburg, B.L. (1989) Am. J. Physiol. 257, L163–L173.
[22] Prochaska, H.J. and Talalay, P. (1988) Cancer Res. 48, 4776–4782.
[23] Prestera, T., Holtzclaw, W.D., Zhang, Y. and Talalay, P. (1993) Proc. Natl. Acad. Sci. USA 90, 2965–2969.
[24] Itoh, K., Chiba, T., Takahashi, S., Ishii, T., Igarashi, K., Katoh, Y., Oyake, T., Hayashi, N., Satoh, K., Hatayama, I., Yamamoto, M. and Nabeshima, Y. (1997) Biochem. Biophys. Res. Commun. 236, 313–322.
[25] Ishii, T., Itoh, K., Takahashi, S., Sato, H., Yanagawa, T., Katoh, Y., Bannai, S. and Yamamoto, M. (2000) J. Biol. Chem. 275, 16023–16029.
[26] Bannai, S. (1984) J. Biol. Chem. 259, 2435–2440.
[27] Deneke, S.M., Baxter, D.F., Phelps, D.T. and Fanburg, B.L. (1989) Am. J. Physiol. 257, L265–L271.
[28] Freeman, M.L., Borrelli, M.J., Syed, K., Senisterra, G., Stafford, D.M. and Lepock, J.R. (1995) J. Cell. Physiol. 164, 356–366.
[29] McDuffee, A.T., Senisterra, G., Huntley, S., Lepock, J.R., Sekhar, K.R., Meredith, M.J., Borrelli, M.J., Morrow, J.D. and Freeman, M.L. (1997) J. Cell. Physiol. 171, 143–151.
[30] Freeman, M.L., Huntley, S.A., Meredith, M.J., Senisterra, G.A. and Lepock, J. (1997) Cell Stress Chaperones 2, 191–198.